Development of Plate Heat Exchangers as Main Components of an Absorption Chiller

Thomas Hasenöhrl

Thesis for the Degree of Master of Science

Division of Heat Transfer
Department of Energy Sciences
Faculty of Engineering, LTH
Lund University
P.O. Box 118
SE-221 00 Lund
Sweden

Division 1: Technology for
Energy Systems and
Renewable Energy
Bavarian Center for Applied
Energy Research e.V.
Walther-Meißner-Str. 6
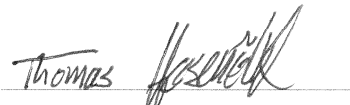85748 Garching
Germany

ZAE BAYERN

Declaration of Authorship

Hereby, I formally declare that I myself have written the enclosed thesis *Development of Plate Heat Exchangers as Main Components of an Absorption Chiller* independently. I did not use any sources or means without to declare them in the text. Any thoughts from others or literal quotations are clearly marked.

This thesis has not been published. It was submitted both to the Technische Universität München and Lunds Tekniska Högskola, according to the terms of the TIME double degree program.

Garching, 20/May/2011

Thomas Hasenöhrl

Abstract

Absorption chillers are energy saving, but low-capacity applications are not available yet. To become competitive with the established vapor-compression chillers, compact and inexpensive main component heat exchangers are required. In the respective capacity range, the conventionally used tube bundle heat exchangers can hardly fulfill that requirement - plate heat exchangers, however, could. The present work evaluates cycle and heat exchanger concepts for a four kilowatt lithium-bromide absorption chiller based on compact plate heat exchangers. The preliminarily planned external temperatures are 15/10°C, 30/38°C and 90/80°C.

Cycle calculations show: Recirculation provides enough solution to permit good wetting of the absorber. Two concepts perform similarly. At the generator, recirculation requires an additional pump. Alternatively, the generator could operate as a pool-generator, but only if the external temperatures are adopted. Making evaporator/absorber and condenser/generator pairwise equal in size results in a low overall heat exchanger area increase. Consequently, two heat exchangers can be pressed on one plate, which lowers the cost and allows to make the chiller more compact.

CFD-simulations of different plate heat exchangers show: Lowering the plate width, which is favorable as to vapor pressure loss, hardly impacts the water side. Rotating the channels towards the horizontal promises better wetting on the solution side, but increases the pressure loss on the water side. Smaller channels between the water channels supposedly increase wetting, too. Moreover, they increase the heat exchange performance and reduce the pressure loss on the water side.

Integrating the wall of the pressure vessel and the solution distribution system into the heat exchanger plates is an approach to further reduce the manufacturing costs and size of the absorption chiller.

Contents

List of Figures

List of Tables

Symbols

Latin characters

Symbol	Unit	Meaning
A	m^2	area
c_p	$\frac{kJ}{kg \cdot K}$	specific heat capacity
C	W	heat capacity rate
COP	$-$	coefficient of performance
f	$-$	solution circulation ratio
f_R	$-$	solution recirculation ratio
h	$\frac{W}{m^2 K}$	heat transfer coefficient
h	m	height
k	$\frac{W}{m \cdot K}$	thermal conductivity
$lmtd$	K	log mean temperature difference
m	$\frac{kg}{s}$	mass flow rate
m_{spec}	$\frac{kg}{m^2 s}$	specific mass flow rate
n	$-$	integer number of heat exchanger plate pairs
p	bar	pressure
q	$\frac{W}{m^2}$	heat transfer rate
Q	W	heat flow rate
s	m	thickness
t	$°C$	temperature
T	K	temperature
U	$\frac{W}{m^2 K}$	overall heat transfer coefficient
v	$\frac{m^3}{kg}$	specific volume
$\dot{V}$	$\frac{l}{s}$	volume flow rate
W	W	mechanical work
x	$-$	solution concentration (mass share of absorbent)

Greek characters

Symbol	Unit	Meaning
Δp	$mbar$	pressure loss
Δt	K	temperature spread
η	$-$	ratio of component performance and cooling performance
ρ	$\frac{kg}{l}$	density

Subscripts

Subscript	Meaning
0	referring to the evaporator (pressure or temperature level)
1	referring to the condenser/absorber (pressure or temperature level)
2	referring to the generator (pressure or temperature level)
a	outlet
abs	absorber
c	cooling water
con	condenser
e	external
$evap$	evaporator
f	film (i.e., falling film)
$flooded$	referring to the flooded part of the generator
gen	generator
i	inner / internal
i	inlet
i	index for discretization
min	minimum
mix	mixed solution

mixed	referring to the mixed recirculation concept
o	outer
package	referring to one plate package
p	plate
pool	for pool boiling
recirc	recirculated
refr	refrigerant
rich	rich solution (high water content)
sat	saturation
sol	solution
sump	referring to the sump recirculation concept
total	all heat exchangers
w	wetted

Abbreviations

Subscript	Meaning
CAD	Computer-Aided Design
CFD	Computational Fluid Dynamics
EES	Engineering Equation Solver (Software for numerical solution of equation systems)
HW	hot water
LiBr	lithium-bromide
OECD	Organization for Economic Cooperation and Development
ZAE Bayern	Bayerisches Zentrum für Angewandte Energieforschung - Bavarian Center for Applied Energy Research

1 Introduction

One reliable source of energy is not even close to being depleted: Simply saving it may be the safest and cleanest option mankind has.
[Jung (2007)]

1.1 Background: The Need for a Sustainable Energy Supply

To be exact, *saving energy* is not a *source of energy*. In fact, coal, gas, uranium and so on are not either - they are rather energy storages, containing energy in a chemical form. And, according to the First Law of Thermodynamics, this chemical energy can be transformed into other forms of energy, for example thermal, mechanical, or electrical energy. But energy can neither be created nor destroyed. For a long time, natural energy resources were considered virtually inexhaustible. Maybe this is why the expression *energy source* could establish in everyday and scientific language. Everybody uses terms like *energy consumption*, *energy conservation* and *energy wastage* - although they are physically incorrect - because there is a general consensus on the meaning of these terms.

Today, it is considered as a matter of fact that natural resources are finite, yet the growing world population and increasing consumption of goods and energy require more and more natural resources. This year, the world population reaches seven billion[1] and in 2030, more than eight billion people will live on earth. The OECD[2] estimates that in the meantime, the world energy consumption will rise by more than fifty percent and the electricity consumption will double [Bethge & Wüst (2007)]. It is only a matter of time until the increased thirst for energy will result in the depletion of the fossil energy resources. If then, however, our civilization still depends on these resources in the way it does today, international conflicts are more than probable. Moreover, the rising consumption of fossil fuels is connected with environmental problems and climate change.

Shortly, the current situation and future prospects demand for a reduced consumption of fossil fuels and, more general, a sustainable energy supply. In Germany and other European countries, the most frequently discussed approach for a sustainable energy supply is a massive extension of the renewable energies. Increasing the renewable energies' share of the overall energy supply, however, is easier and faster to achieve if the overall energy consumption is lower. Insofar, [Jung (2007)] is right when he states that saving energy is an energy source. Saving energy helps to achieve a sustainable energy supply because it reduces the number of wind turbines, biogas plants, solar panels, and so on, that need to be installed to replace the conventional power and heat facilities with sustainable alternatives.

---

[1] [Kommer & Hinz (2010)]
[2] Organization for Economic Cooperation and Development

1.2 Market Gap for Low-scale Absorption Chillers

One sector in which considerable amounts of power can be saved is air conditioning. In Germany, air conditioning in the residential sector is not established yet. It is mostly business and office premises that are equipped with air conditioning. In other countries, however, air conditioning plays a more important roll [Clausen (2007)]. In the United States, for example, virtually all buildings are air conditioned - including residential buildings. Unsurprisingly, this also reflects in the country's power consumption: More than ten percent of the power consumed in the United States is used for air conditioning. On hot days, that share may rise up to more than twenty percent [Höges (1997)]. Worldwide, the market for air conditioners is growing. Hence, also the energy consumed for air conditioning increases [Clausen (2007)].

Currently, most air conditioning systems with medium capacity and all air conditioners with low capacity are based on the vapor-compression technology. These vapor-compression chillers are usually driven by an electric compressor and consume a considerable amount of electric power, the most valuable form of energy. There is, however, another technology for chill production whose driving energy is not electric power but heat: absorption chilling. Depending on their design, absorption chillers can use different heat sources, for instance district heat, reject heat or solar heated water - heat that is either abundant or can be produced in an inexpensive and ecologically sustainable way. Estimations for the primary energy saving by absorption chillers are as high as 40 to 60 percent [Clausen (2007)]. That makes absorption chillers a promising alternative to vapor-compression chillers.

All the same, private customers cannot buy absorption chillers. Most absorption chillers on the market have capacities of hundred kilowatts and more - far too much for chilling an apartment or a single-family home. In fact, there is no absorption chiller in the capacity range that is relevant for the residential sector, that is, below ten kilowatts. The reason for that market gap is of technical and economical nature:
The main components of an absorption chiller are heat exchangers. In conventional absorption chillers with capacities of hundred kilowatts and more, these heat exchangers are tube bundle heat exchangers. As for other technologies, downscaling tube bundle heat exchangers does only work to a certain extent. The relative size, weight, material cost and labor cost for the tube bundle heat exchangers increase. Consequently, a chiller with low capacity, having small tube bundle heat exchangers, becomes large, heavy and expensive compared to its capacity and, above all, compared to vapor-compression chillers with the same capacity. For absorption chillers with low capacities, tube bundle heat exchangers are therefore not the right technology [Estiot (2009)].

1.3 Motivation and Structure of this work

Some years ago, the *ZAE Bayern*[3] started to research on alternative heat exchanger technologies for low-scale absorption chillers. The goal of this research is to develop a compact and inexpensive heat exchanger that allows to design low-scale absorption chillers able to establish on the market, which is dominated by the conventional vapor-compression chillers. During that research, plate heat exchangers turned out to be a promising approach. The first prototype, however, did not perform as expected, mainly because of poor wetting with solution.

Last year, the ZAE Bayern launched a project that aims at the development of a low-capacity absorption chiller with compact plate heat exchangers. The first and central task is to improve the plate heat exchanger design. Good wetting, a compact geometry and a low first cost are the aspired qualities of the new plate heat exchanger.

The previous work on the project has brought about a number of ideas for how to change the heat exchanger and cycle design in order to attain these qualities. However, some of these ideas need to be investigated more deeply to make sure that the respective design changes in fact have a positive impact. This investigation is provided by the present work:

First, chapter 2 introduces some fundamental knowledge on vapor-compression chillers and absorption chillers. Then, chapter 3 briefly discusses the use of tube bundle and plate heat exchangers in absorption chillers and presents the integration design concept as an approach to create a compact, low-cost plate heat exchanger. The cycle calculations in chapter 4 and the flow simulations in chapter 5 evaluate the different ideas for design changes. Lastly, chapter 6 summarizes the most important findings and their consequences for the heat exchanger and cycle design.

---

[3]Bayerisches Zentrum für Angewandte Energieforschung - Bavarian Center for Applied Energy Research

2 Fundamentals of Absorption Chilling

This chapter introduces some fundamentals that are helpful for the reader who is not familiar with the topic absorption chilling. More comprehensive information is available in the referenced literature.

2.1 Vapor-Compression Chiller

Figure 2.1 schematically shows a vapor-compression chiller. The main components are an evaporator, a condenser, a compressor and a throttle. The compressor increases the pressure level of the refrigerant - for instance, ammonia or water - vapor from p_0 to p_1. For p_1, the refrigerant condenses at the temperature T_1, somewhat above the rejection temperature of the heat sink. For an ordinary refrigerator and many air conditioners, the heat sink is the ambient air. Thus, the rejection temperature must be above the ambient temperature, so that the heat transport from the condenser to the ambient air works. Having condensed, the now liquid refrigerant flows down to the evaporator - through the throttle, which reduces the refrigerant pressure from p_1 to p_0. In the evaporator, the refrigerant evaporates at a temperature T_0 lower than T_1, absorbing heat from the chilled water used for air conditioning or from the interior of a refrigerator, for instance. The refrigerant vapor then is compressed again, and so on.
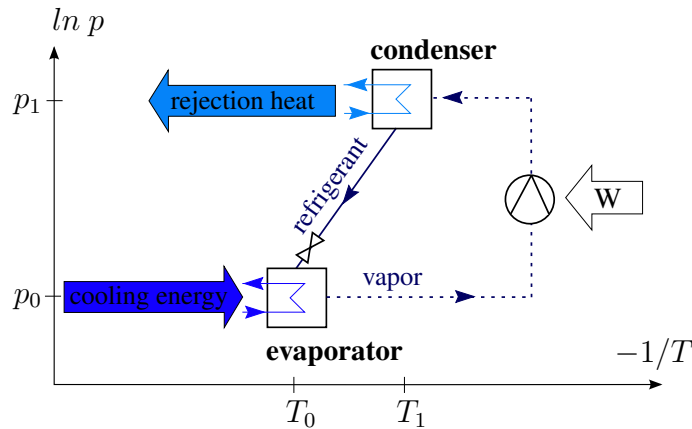

Figure 2.1: Schematic of a vapor-compression chiller

For compressing the refrigerant vapor, the compressor has to provide the mechanical work W:

$$W = m \int_0^1 v(p, T) dp. \tag{1}$$

The work that could be extracted from the expansion process is negligible because the expanded refrigerant is liquid and hence virtually incompressible. Yet, the compression

work W is not negligible. Usually, and particularly in refrigerators and in small scale air conditioning applications, the compressor is driven by an electric motor. Consequently, these vapor-compression chillers consume a significant amount of electricity ([Alefeld & Radermacher (1993)], [Herold et al. (1996)]).

2.2 Absorption Chiller

In absorption chillers, the compressor used in vapor-compression chillers is replaced by a so-called thermal compressor: A solution absorbs the refrigerant vapor and is then pumped to the upper pressure level, where the refrigerant desorbs from the solution to condense and eventually expand.

Hence, absorption chillers do not only need a fluid that works as refrigerant; absorption chillers require a fluid pair, an absorbent and a refrigerant. Besides a high affinity between the refrigerant and the absorbent, a desirable property of the working pair is that the absorbent has a low vapor pressure compared to the refrigerant. There are, however, numerous desirable properties for working pairs, and some of them are mutually exclusive. Hence, the choice of the working pair is a compromise and depends inter alia on the kind of application and the resulting temperature levels. The most prominent fluid pairs used for absorption chillers are ammonia and water, and water and lithium-bromide (LiBr) ([Alefeld & Radermacher (1993)], [Herold et al. (1996)]).

Figure 2.2 depicts a schematic of a single-effect absorption chiller. The chiller consists of the main components evaporator, absorber, generator and condenser. A fifth heat exchanger, the solution heat exchanger, is usually applied to improve the process efficiency. The absorber and the condenser have to be cooled, whilst the generator needs to be provided with driving heat. The heat taken up by the evaporator corresponds to the cooling energy produced by the absorption chiller.

The main components' positions in the schematic qualitatively correspond to the respective temperature and pressure levels. Inside the evaporator and the absorber the pressure is virtually equal, p_0. Also the generator and the condenser have the same pressure level, p_1. The pressure level p_1 is higher than p_0. Moreover, there are three temperature levels, T_0 for the evaporator, T_1 for absorber and condenser, and T_2 for the generator. The positions of all other components do not necessarily reflect the respective pressure and temperature levels.

Note that the rejection heat from the condenser and absorber can also have different temperature levels, depending on the design of the cooling system. In the example of figure 2.2, the cooling water first flows through the absorber and then through the condenser. Consequently, the temperature levels are quasi the same, even though the cooling water is already heated in the absorber and hence enters the condenser with a slightly higher temperature than the absorber. In other cycles, the cooling water first flows through the condenser and then through the absorber. The two components can also have separate cooling cycles. The present work however only considers the variant shown in figure 2.2.
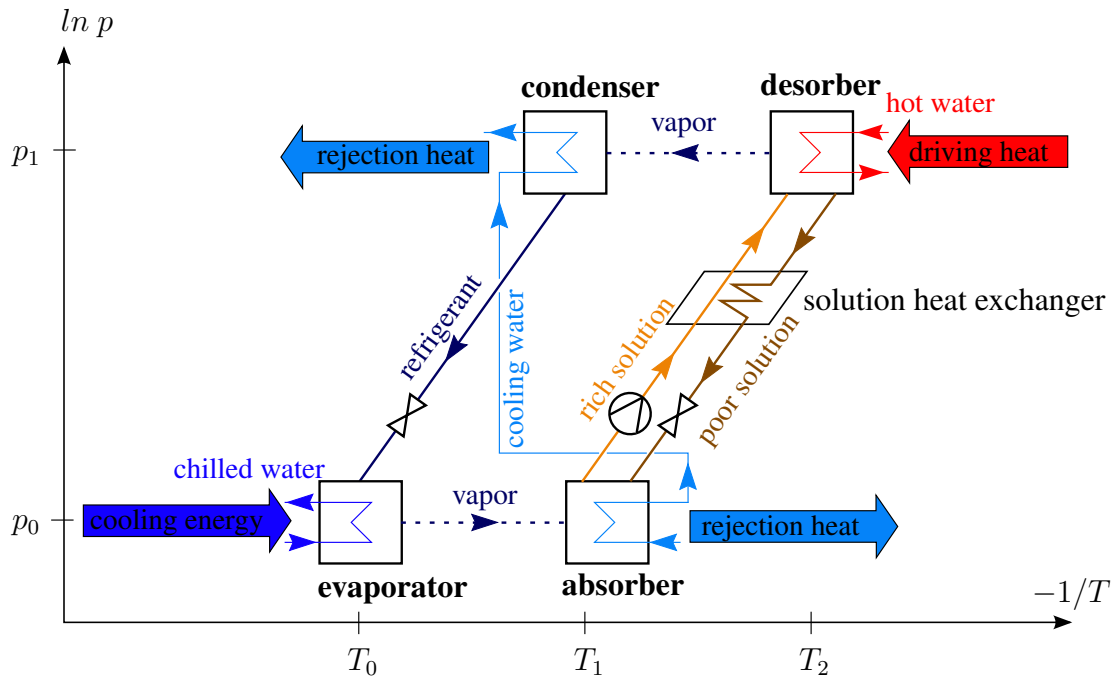
Figure 2.2: Schematic of a single-effect absorption chiller (adopted from [Estiot (2009)])

Briefly, the function of the absorption cycle can be described as follows: In the evaporator, the refrigerant, coming from the condenser, evaporates at the pressure level p_0. As p_0 is low, the refrigerant evaporates at a low temperature level, T_0. The chilled water loop provides the necessary heat. The refrigerant vapor produced in the evaporator then flows to the absorber, where it is absorbed by a liquid film of poor working solution, yielding rich solution and rejection heat at the temperature level T_1. *Poor* and *rich solution* indicate solution containing little and much refrigerant, respectively. Pumped to the generator, the rich solution is boiled at the pressure level p_1. As the pressure p_1 is higher than p_0, also the saturation temperature, that is, boiling temperature, T_2 of the solution in the generator is higher than the temperature T_1 of the absorption process. Having a higher vapor pressure than the absorbent, only refrigerant evaporates and flows to the condenser. The remaining solution is poor in refrigerant and flows through an expansion valve back to the absorber to again absorb refrigerant vapor. In the condenser, the vapor is cooled and condenses. Finally, the refrigerant condensate flows through an expansion valve back to the evaporator, where it evaporates again.

As mentioned above, the evaporation heat provided by the chilled water loop corresponds to the capacity of the absorption chiller. The cooling water temperature increases as the cooling water absorbs the condensation and absorption heat. In a cooling tower, it can reject that heat to, for instance, the ambient air. Hot water provides the driving energy for the absorption cycle. Various sources for the hot water are possible, for instance combustion, industrial waste heat, reject heat from power generation or solar collectors. In any case, the heat capacity rates and the temperature levels of

the external fluids have to match the cycle design ([Alefeld & Radermacher (1993)], [Herold et al. (1996)], [Schweigler (1999)]).

T_2, the temperature in the generator, is higher than T_1, the temperature in the absorber. Consequently, also the poor solution leaving the generator is warmer than the absorber and has to be cooled to T_1 after entering the absorber. In the same way, the rich solution leaving the absorber is cooler than the generator and must be heated to T_2 after entering the generator. To reduce these heating and cooling loads, a solution heat exchanger as sketched in figure 2.2 is usually applied to transfer heat from the poor solution to the rich solution. Thus, the temperature difference between the internal temperature of the generator and absorber and the respective solution entering them is reduced. This reduction in required driving heat results in a better overall efficiency of the absorption chiller.

The common figure to express the efficiency of absorption chillers is the *coefficient of performance (COP)*, defined as

$$COP = \frac{driving\ heat}{cooling\ energy}.$$

(2)

For a certain cooling capacity, the required driving heat input determines the COP. Hence it becomes obvious that a solution heat exchanger, reducing the driving heat input, increases the COP. Another commonly used figure is the *solution circulation ratio f*, defined as the ratio of the respective mass flow rates of the rich solution and the refrigerant:

$$f = \frac{m_{rich}}{m_{refrigerant}}.$$

(3)

By definition, f is larger than one, and commonly it ranges between ten and twenty-five.

A more abstract but common way to depict absorption cycles is the Dühring-plot, as shown in figure 2.3 for the working pair water and lithium-bromide (LiBr). The saturation temperature, that is, boiling temperature, of the solution is given on the x-axis, the corresponding dew-point temperature of water, the refrigerant, on the left y-axis and the corresponding dew-point pressure of water on the right y-axis. The gray lines are isosteres, lines of constant solution concentration. The water vapor pressure is a function of both the temperature and the solution concentration. With the isosteres, both interdependencies can be plotted in one diagram: Each isostere shows the solution's equilibrium states for a certain LiBr concentration. The light blue line represents pure water and the light red line marks the solubility limit of LiBr in water.

Figure 2.3 also depicts a single-effect absorption cycle as described above and illustrated in figure 2.2. Figure 2.3 however is quantitative as to the temperatures and pressure levels in the main components evaporator, absorber, generator and condenser.
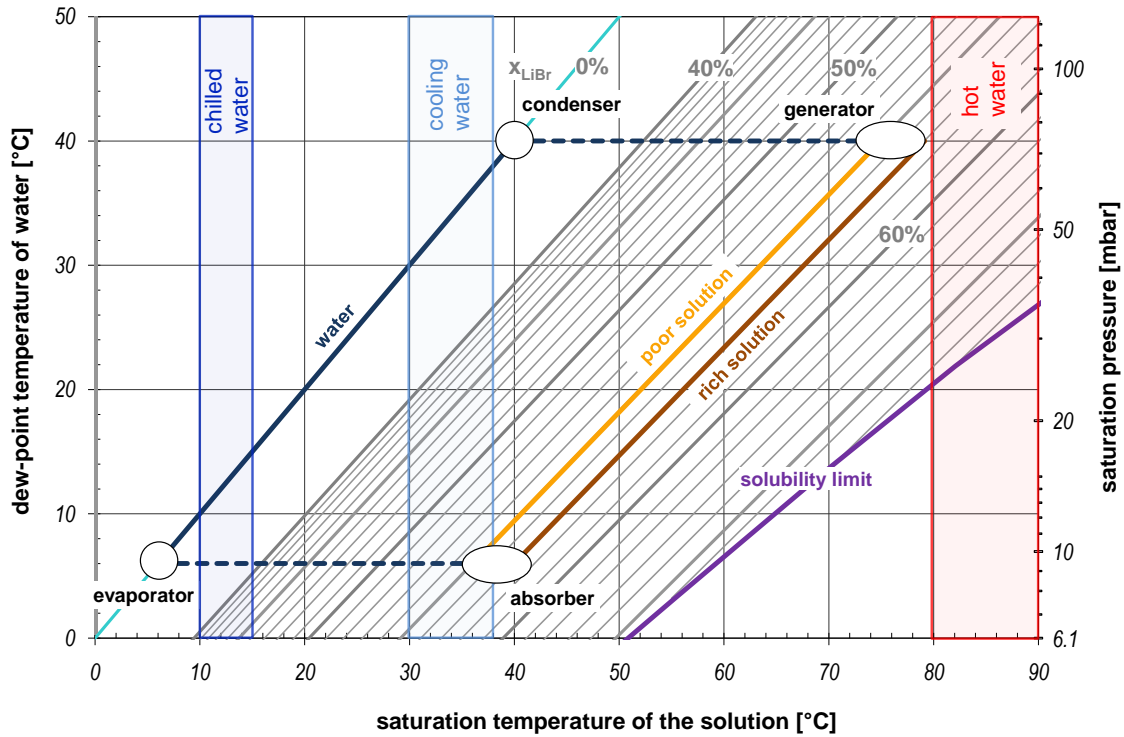
Figure 2.3: Single-effect absorption cycle in a Dühring-plot

Moreover, the diagram contains thinkable external temperatures, that is, the inlet and outlet temperatures of the chilled water, the cooling water and the hot water, respectively. The external temperatures are represented by the dashed lines. As heat transport requires temperature gradients, the hot water and chilled water temperatures are above the generator and evaporator temperature, respectively, and the cooling water temperature is below the condenser and absorber temperature.

The single-effect absorption chiller is the simplest kind of absorption chiller. Various kinds of more sophisticated cycles are described in the literature. For the present work, however, only the single-effect cycle is of interest.

3 Heat Exchangers for Absorption Chillers

Although not literally mentioned in the previous elaborations on the vapor-compression and the absorption chiller, the main components of these applications are heat exchangers. Currently, the heat exchangers in most absorption chillers are horizontally arranged tube bundle heat exchangers operating in falling film mode. On top of the heat exchangers, the refrigerant or the solution, respectively, is applied to the outside of the tubes and forms a falling film - in the condenser, the condensed refrigerant vapor forms the falling film. Inside the tubes flows the chilled water, cooling water, or hot water, respectively. Figure 3.1(a) depicts the sketch of a falling film tube bundle absorber. Regardless of the kind of heat exchanger used, there is always one side with water and one with vapor and cooling agent or solution. The former is named *water side*, the latter *film side* or *vapor side*, respectively. *Film side* and *vapor side* are synonymous, their use mostly depends on the context.

(a) Tube bundle heat exchanger   (b) Plate heat exchanger
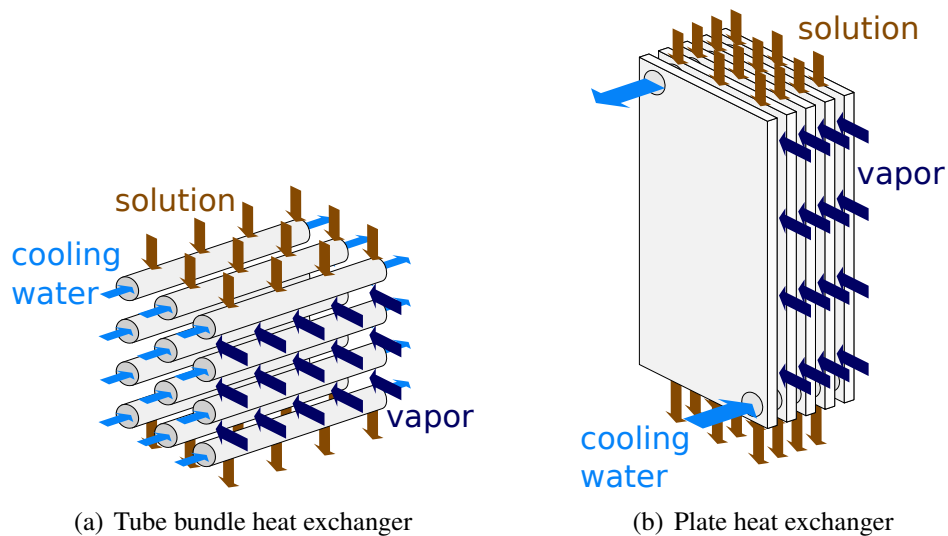
Figure 3.1: Heat exchangers used as absorbers

3.1 Disadvantages of Small Tube Bundle Heat Exchangers

At present, absorption chillers are only established for capacities in the range of hundreds of kilowatts and more. The present work however is part of the project *Absorptionskältemaschine auf Basis kompakter Plattenapparate* (absorption chiller with compact plate heat exchangers), which aims at the development of a three to five kilowatt water/LiBr absorption chiller. For that low capacity range, the chiller requires small heat exchangers. The simplest approach would now be to downscale the tube bundle

heat exchangers used in the established absorption chillers of medium capacity to the required sizes. This approach has however proved unfavorable, mostly for cost reasons.

Water/LiBr chillers operate at total pressures well below one hundred millibars, that is, far below the ambient air pressure. Air entering the chiller results in a performance decrease because the pressure inside the chiller increases and, in the presence of LiBr, air causes corrosion, which shortens the chiller's life cycle. Hence, it is important to prevent the ambient air from entering the heat exchangers and hence the chiller.

To make the tube bundle heat exchangers pressure tight, each tube has to be mated thoroughly into the tube sheets holding the tubes, which requires a labor-intensive manufacturing step. The height of the tube bundle determines the residence time of the solution on the heat exchanger surface and thus also the amount of vapor that it can absorb and eventually the concentration difference between the rich and the poor solution - an important parameter for the cycle design. In order not to reduce the concentration difference between rich and poor solution, the tube bundle height, that is, the number of horizontal tube layers should keep constant when the heat exchanger is downscaled. The number of vertical tube layers, however, can decrease. But for a significant reduction of the heat exchanger area, this will not be sufficient - the tubes have to become shorter. For shorter tubes however, the relative labor cost for the heat exchanger assembly increases.

In addition, the tube sheets have to be rather thick to withstand the prevailing pressure difference and to allow for mating the tubes in a pressure-tight way. For medium and large-scale absorption chillers with large heat exchangers, these aspects are not weighty, yet they are for small-scale chillers. As the material and particularly the labor costs do not correlate linearly with the chiller capacity, the first cost for a small-scale chiller with tube bundle heat exchangers is unproportionally high ([Estiot (2009)]).

3.2 Plate Heat Exchangers for Absorption Chillers

To avoid the disadvantages of using tube bundle heat exchangers for the planned small-scale absorption chiller, the goal of the project *Absorptionskältemaschine auf Basis kompakter Plattenapparate* is to develop an absorption chiller with plate heat exchangers as main components.

Plate heat exchangers usually consist of pressed metal sheets. Their manufacture requires a machine press with a die and a punch, having the negative pattern of the desired plate pattern on the respective side. The sheet is put on the die and then the punch presses it against the die, forcing it to deform into the desired shape. Die and punch have to be hardened, hence tool costs for pressing are high. The variable costs, however, are low compared to tube bundle heat exchangers. Therefore, plate heat exchangers are an inexpensive alternative when produced in large numbers. Moreover, plate heat exchangers are more compact than tube bundle heat exchangers: For the same heat transfer capacity, a plate heat exchanger is smaller than a tube bundle heat exchanger.

Figure 3.2(a) depicts a set of typical heat exchanger plates. A stack of such plates forms a heat exchanger, where the two fluids alternately flow in every second gap between two adjacent plates. A cut brazed plate heat exchanger is shown in figure 3.2(b). It has a large opening for the one, and a smaller opening for the other fluid. In contrast to gasketed plate heat exchangers, brazed plate heat exchangers have a good pressure and vacuum tightness. Therefore, they can be used in air conditioning applications, where the operating pressure usually differs notably from the ambient pressure. Figure 3.1(b) schematically shows a plate heat exchanger operating as a falling film absorber.

(a)   (b)

Figure 3.2: Heat exchanger plates (a) and a cut open brazed plate heat exchanger (b) [Alfa Laval (2004)]

In a previous project, [Estiot et al. (2007)], [Behr (2006)] and [Hulin (2008)], investigated a plate heat exchanger operated as absorber. Characteristic for their plate heat exchanger: The film side is open at the edges. On the one hand, that allows the vapor to enter or exit the heat exchanger, respectively, and to apply solution from above the heat exchanger to attain a falling film. On the other hand, that kind of plate heat exchanger requires a vacuum vessel, because subatmospheric operating pressures are required, and a solution application system, analogously to a tube bundle heat exchanger. Estiot, Behr and Hulin found that the plate heat exchanger performed worse than expected because surface wetting with solution on the plates was poor. Hence, one major goal of the current project is to design heat exchanger plates with improved surface wetting.

3.3 Advanced Plate Design: Integration

As section 3.2 shows, using plate heat exchangers instead of tube bundle heat exchangers is a promising approach in designing a compact and inexpensive low-capacity absorption chiller. Moreover, another design approach for heat exchangers arose during the current project, a design approach with high potential to reduce cost, weight and size of the absorption chiller: Integration. This section presents the idea to integrate (1) the solution distribution system and (2) the walls of the vacuum vessel into the plate and (3) two heat exchangers on one plate. These three integration concepts can be implemented either altogether or only one or two of them.

3.3.1 Integrating the Fluid Distribution System

Falling film heat exchangers require a system to distribute the liquid - be it the cooling agent or the solution. So far, nozzles or other external systems located above the respective heat exchanger have been used to apply the solution on the heat exchangers. These distribution systems and the necessary piping increase both the material cost and the labor cost of the chiller - especially for small-scale chillers.

Integrating the solution distribution system into the plates, however, cuts these costs. The plate integrated distribution system is manufactured in the same moment as the heat exchanger plates are stamped and assembled. Consequently, it does, unlike external distribution systems, not require any extra labor and no extra parts. Moreover, it allows for a very compact design.

Besides the inlet and outlet openings for the external fluid, the integrated distribution system has additional inlet and outlet openings for the solution or refrigerant, respectively. When used as an absorber, the heat exchanger works as follows: From the inlet opening, located at the top of the plate, the poor solution flows into the distribution system, for example a horizontal channel, in which it spreads on the entire width of the heat exchanger. Then the solution forms a falling film flowing downwards and absorbing water vapor. After reaching the bottom of the heat exchanger, the solution is collected and leaves the heat exchanger through the outlet opening to be pumped to the generator.

When used as a generator or evaporator, the heat exchanger works correspondingly - with desorption and evaporation instead of absorption, respectively. When used as a condenser, the distribution system is not necessary, but it does not constrain the condensation. Hence the same type of heat exchanger can also be used as a condenser.

3.3.2 Integrating the Vacuum Vessel

As the lithium-bromide absorption chiller requires subatmospheric pressures, the heat exchangers have to be inside pressure-tight vessels. Because of the very low inside pressure, the vessels have to meet high quality standards and their manufacturing is costly.

But in contrast to tube bundle heat exchangers, plate heat exchangers can form their vessel themselves. In fact, conventional plate heat exchangers do not need a pressure vessel, because their volumes for both fluids are hermetic. The Estiot et alii plate heat exchangers, however, is open on the solution side and does therefore need a pressure vessel. Yet, if the solution distribution system is integrated in the plates, the solution side can be closed again. Roughly, this works similarly as for conventional plate heat exchangers:

When dimensioning the raw plate for the heat exchanger larger than the heat exchanger actually requires, pressing produces a heat exchanger with an enlarged edge. Edging this surplus edge forms a pan like object where the heat exchanger is located at the bottom. When assembling the heat exchanger plates as usually, the edged sections of the plates form the vacuum vessel. Every other plate has to be turned over so the water sides and the vapor sides of the adjacent plates are in contact. Consequently, the edging direction of the plate edges has to alternate, too.

A plate-integrated vessel supposedly is the most compact and light-weight vessel that can be realized. Moreover, compared to a conventional vacuum vessel, its manufacture is significantly faster and less expensive.

3.3.3 Integrating Two Heat Exchangers on One Plate

Pairwise equal heat exchangers can be made on one and the same plate. Consider figure 3.3, depicting the sketch of a plate with the pattern for two equal heat exchangers. Such a *two-in-one* heat exchanger plate must be symmetric as to the fluid inlet and outlet openings, whereas the channel pattern of the right heat exchanger is a translation of the left one. Thus, when two plates are assembled to a plate package - one of them has to be turned over around the center line first -, the corresponding fluid openings coincide and hence allow for the necessary fluid flow to and from the adjacent plate packages.

The channels form the cavity system in the same manner as they do for conventional, *single*, heat exchangers. That means that the cavities for the external fluid form a closed system - with exception for the inlet and outlet openings - and that the vapor side is open. Consequently, vapor can flow from one to the other heat exchanger - the vapor piping can be omitted and the distances for the vapor to flow are short. Just as the integration of the distribution system, omitting the vapor piping results in a simpler and cheaper assembly and lower material cost. And the short distances for the vapor flow result in low pressure loss, which is favorable, too - see section 5.1.

Another advantage of two-in-one plates is that the fluid inlet and outlet openings do not have to be located in the center, even though a plate package consists of two identical plates. Thanks to the symmetrical arrangement on the left and the right heat exchanger, the respective openings coincide in spite. The openings for external and internal fluid do not have to be placed on top of each other, which would result in increased unused areas on the top and the bottom of the heat exchanger, where only one of the fluids would be
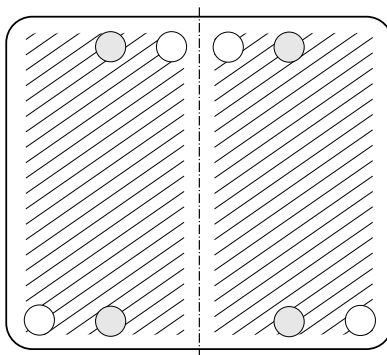
Figure 3.3: Two-in-one heat exchanger plate. The circles with gray filling are the inlet and outlet
openings for one fluid, the circles with white filling for the other fluid. All openings are
positioned symmetrically to the center line (dot-dashed line). The channel pattern
(indicated by the parallel lines) on the right is a translation of the channel pattern
on the left. Assembling this kind of plates gives two identical heat exchangers.

present. On the two-in-one plate, however, the openings for the internal and the external
fluid can have the same vertical position and be placed side by side, for instance. That
allows for a more compact design.

The calculations in section 4.2 evaluate how using pairwise equally sized heat exchang-
ers impacts the overall heat exchanger area of the planned absorption chiller.

4 Modeling of Absorption Chiller Cycle Concepts

The present work is a step in the engineering of a new absorption chiller that uses plate heat exchangers as main components. The chillers' planned capacity is four kilowatts; table 4.1 lists the planned external temperatures. The intention is to design an absorption chiller that can use water heated with reject heat from a combined heat and power plant or water heated by solar collectors. These heat sources can heat water to rather moderate temperatures. Therefore, the respective hot water is called *low temperature hot water*. A typical temperature level of low temperature hot water is ninety degrees Celsius. Thus, the planned inlet temperature for the hot water is ninety degrees Celsius. The planned cooling water inlet temperature is thirty degrees Celsius because that comparably high cooling water temperature requires a smaller cooling tower than a lower cooling temperature, as, for instance, 27 degrees Celsius. And moreover, thirty degrees Celsius may even be reached with a dry cooling tower, which is easier to install and less expensive than a wet cooling tower. Lastly the chilled water inlet and outlet temperature is fifteen and ten degrees, respectively - suitable for air conditioning.

Table 4.1: Planned external temperatures for the absorption chiller

temperatures $[°C]$	inlet	outlet
chilled water	15	10
cooling water	30	38
hot water	90	80

This section presents a number of results from numerical cycle calculations. The goal of these calculations is to evaluate different cycle designs and to give an idea of the required heat exchanger areas and the achievable coefficient of performance (COP). Moreover, the calculations show whether the planned external temperatures are adequate for the planned cycles - here, especially the use of a pool generator is critical, as section 4.3 will show.

In the mathematical model, an equation system consisting of energy, mass and salt balances in the main components evaporator, absorber, generator and condenser, and in the solution heat exchanger, describes the absorption chiller cycle. The commercial software *Engineering Equation Solver* (EES) solves the equation system. Moreover, EES provides a library with the relevant physical properties of water and aqueous lithium bromide solution, the two substances present in the absorption chiller, the so-called *working pair*. The library is based on data in [Parsons & Forman (1989)] and

[Uemura & Hasaba (1964)].
The cycle models are based on the following assumptions and simplifications[4]:

- The system is in a steady state. That is, the mass flow rate of water vapor absorbed in the absorber is equivalent to the mass flow rate of water vaporized in the generator.

- The pressure drop inside the piping and the vessels is negligible.

- The heat transported between any of the components of the cooling machine and the surroundings is negligible.

- The main component (evaporator, absorber, generator and condenser) heat exchangers and the solution heat exchanger have constant overall heat transfer coefficients U.

- The heat exchangers are fully wetted.

Note that the used U-values have been measured in a ten kilowatt absorption chiller with tube bundle heat exchangers and with similar external temperatures. As no other numbers are available, we assume that the main component heat exchangers and the solution heat exchanger of the modeled cycles have all about the same overall heat transfer coefficients as the respective heat exchangers of the ten kilowatt chiller: $U_{evaporator} = 1.2$ kW/m^{2}K, $U_{condenser} = 2.0$ kW/m^{2}K, $U_{absorber} = 1.0$ kW/m^{2}K and $U_{generator} = 0.8$ kW/m^{2}K. Tests with prototype heat exchangers will have to show in how far the estimated U-values differ from the real ones.

As stated in the introduction, the specific heat exchanger area is one of the factors defining the costs of an absorption chiller. It is defined as the overall heat exchanger area of the absorption chiller divided by the cooling capacity of the chiller. Moreover, the specific heat exchanger area influences the size of the main components and thus also the size of the entire absorption chiller. As both low costs and a small size of the chiller are favorable, the cycle modeling aims at a minimum heat exchanger area at each calculated operating point. The chiller capacity is four kilowatts for all calculations, hence the calculated absolute heat exchanger areas can easily be transformed into specific areas if the reader is interested in specific areas.

This chapter has the following structure: The first section evaluates two concepts of solution recirculation at the absorber, the second section investigates the impact of using pairwise equally sized heat exchangers for absorber/evaporator and generator/condenser, and the third section examines if the planned external temperatures allow for the use of a pool generator.

---

[4]The first three of these assumptions correspond to the assumptions of [Joudi & Lafta (2000)].

4.1 Modeling of Absorber Recirculation

First, this section answers the question why to consider solution recirculation at the absorber. Then the modeled recirculation concepts are presented, followed by the results of the cycle calculations and their discussion.

4.1.1 Motivation for Absorber Recirculation

Plate heat exchangers do not wet as well as tube bundle heat exchangers. The presumed reason for that drawback is the vertical and continuous geometry. Compared to tube bundles, which have convex surfaces and where solution collects at the bottoms of the tubes before dripping off to the next tube, the solution flows faster on a plate. Therefore, larger solution mass flow rates are necessary to keep up a contiuous film, which results in an efficient use of the plate heat exchanger. The calculation in appendix A estimates the solution mass flow necessary to attain good wetting of the plate heat exchanger previously investigated at the ZAE Bayern. That mass flow rate refers to one plate package, that is, the surfaces of two adjacent plates. The absorber heat exchanger, and the other heat exchangers as well, however, will consist of several, say n, plate pairs.[5] Consequently, the mass flow rate needed for good wetting will be n times as much as the mass flow rate for one package. And so will the area.

Yet, the modeling does not return integer multiples of the plate pair surface area. EES solves the equation system describing an absorption chiller cycle with the task to minimize the overall heat exchanger area. But it does not know what plate size will be used for the heat exchangers,[6] so the returned heat exchanger areas will usually be non-integer multiples of the intended plate surface area and can be seen as a lower limit for the heat exchanger design.

Again, the cycle model is based on the assumption of good wetting. And plate heat exchanger wetting is good when the solution mass flow rate is sufficient. Hence we define a ratio of the solution mass flow rate applied on the absorber and the absorber area; let us name that ratio *specific mass flow rate*. The calculations in appendix A, based on wetting tests by [Beil (2011)], show that the minimum specific mass flow rate for the current heat exchanger design is some 0.15 kg/m^{2}s. The calculated absorber heat exchanger area is only realistic for a specific mass flow rate of at least that value.[7]

In a basic single-effect absorption chiller cycle, the solution mass flow rate applied

---

[5]n is an integer.

[6]In fact, the used equation systems are not limited to the calculation of absorption chillers with plate heat exchangers. They can be used for absorption chillers with any other kind of heat exchanger, as long as the assumptions and constraints of the equation system suit the heat exchanger type in question.

[7]Note that the specific mass flow rate necessary for good wetting depends, inter alia, on the plate width. When changing the plate width notably, an adjustment of the specific mass flow rate will be necessary to keep wetting on a good level. Therefore, the specific mass flow rate could also refer to the mass flow rate per plate width. Both ratios can, however, be transformed into one another.

on the absorber equals the mass flow rate of poor solution coming from the generator. If this mass flow rate is to be increased in order to provide the specific solution mass flow rate necessary for good wetting, more solution circulates between absorber and generator, which is expressed by a rising solution circulation ratio f. The increased solution mass flow rates in turn increases the required pump work and the losses in the solution heat exchanger, both decreasing the overall efficiency of the chiller. Figure 4.1 shows the specific mass flow rate at the absorber as a function of f for the cycle model with the external temperatures given in table 4.1. The graph shows that f must be far beyond the plotted range so the specific mass flow rate reaches the threshold for good wetting. As the discussion in section 4.1.3 shows, for an f far beyond twenty-five, the total heat exchanger area is high, which is the opposite of what we aim at, and the COP becomes really poor, which is unfavorable as well. So, increasing f in order to attain good wetting is not the right approach.
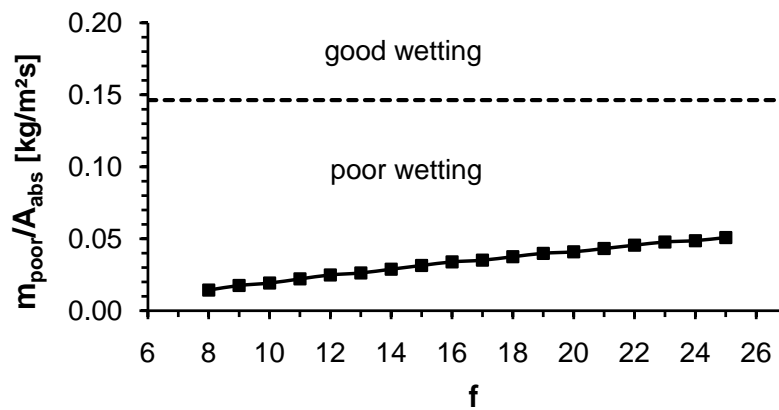
Figure 4.1: Specific solution mass flow rate at the absorber of the basic cycle. The dashed line marks the threshold for good wetting.

However, the specific mass flow rate at the absorber can be independent of the mass flow rate circulating between the absorber and the generator. Solution recirculation at the absorber provides this independence. It allows for an increase of the solution mass flow rate applied on the absorber heat exchanger at constant mass flow rates between absorber and generator. Thus, we can prescribe a constant specific mass flow rate and optimize other variables in the cycle model.

4.1.2 Modeled Recirculation Concepts

The cycle calculations encompass two concepts for solution recirculation at the absorber:

- Mixed recirculation: Rich solution is taken from the absorber sump and mixed with the poor solution coming from the generator. The mixed solution is then

applied on the absorber. See figure 4.2(a).

- Sump recirculation: Rich solution is taken from the absorber sump and applied on the absorber whilst the poor solution coming from the generator enters the absorber sump. See figure 4.2(b).
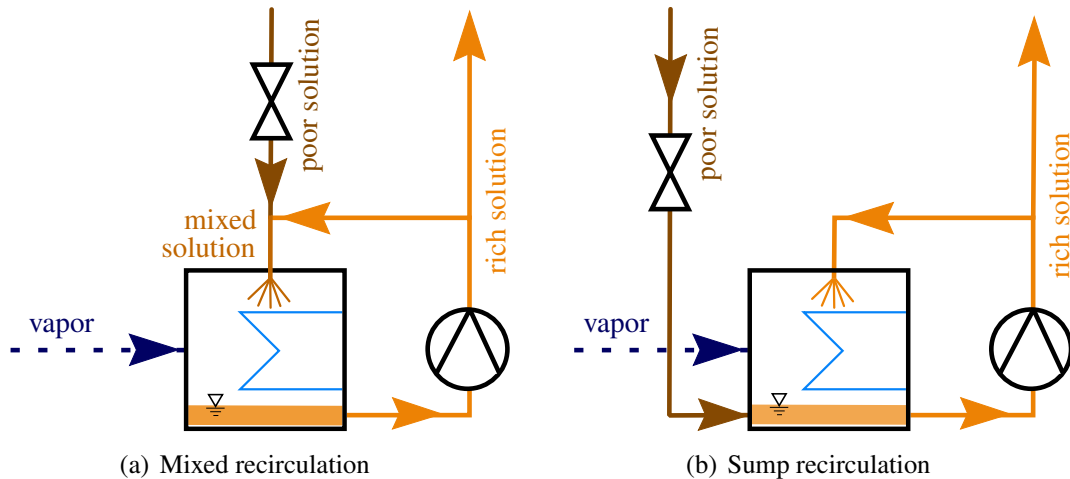

(a) Mixed recirculation

(b) Sump recirculation

Figure 4.2: Modeled concepts for solution recirculation at the absorber

[Schweigler (1999)] describes a third recirculation concept where the poor solution coming from the generator and the recirculated solution from the absorber sump are applied on separate sections of the absorber heat exchanger. That concept performs similar to the mixed recirculation concept. But it is inflexible because the sections where poor and recirculated solution are applied on the heat exchanger are fixed and cannot be adopted at part load. Hence we do not consider that concept any further.

4.1.3 Results of the Absorber Recirculation Cycle Calculations

Before actually discussing the results of the cycle calculations with solution recirculation at the absorber, we have a quick look at the single-effect absorption chiller without recirculation. For the sake of simplicity, let us call this cycle concept *basic cycle*.
Consider figure 4.3. The lowest curve in the graph shows the total heat exchanger area for the basic cycle. After a slight decrease, A_{total} reaches a minimum at a solution circulation ratio of eleven. Then it increases nearly linearly. The upper black line, almost disappearing behind the blue and orange lines, shows the basic cycle's COP. It declines linearly with increasing f. These characteristics of the basic cycle for the overall heat exchanger area and the coefficient of performance correspond to the results of the calculations of, for example, [Wuschig (2007)].
However, the calculation is based on the assumption of constant overall heat transfer
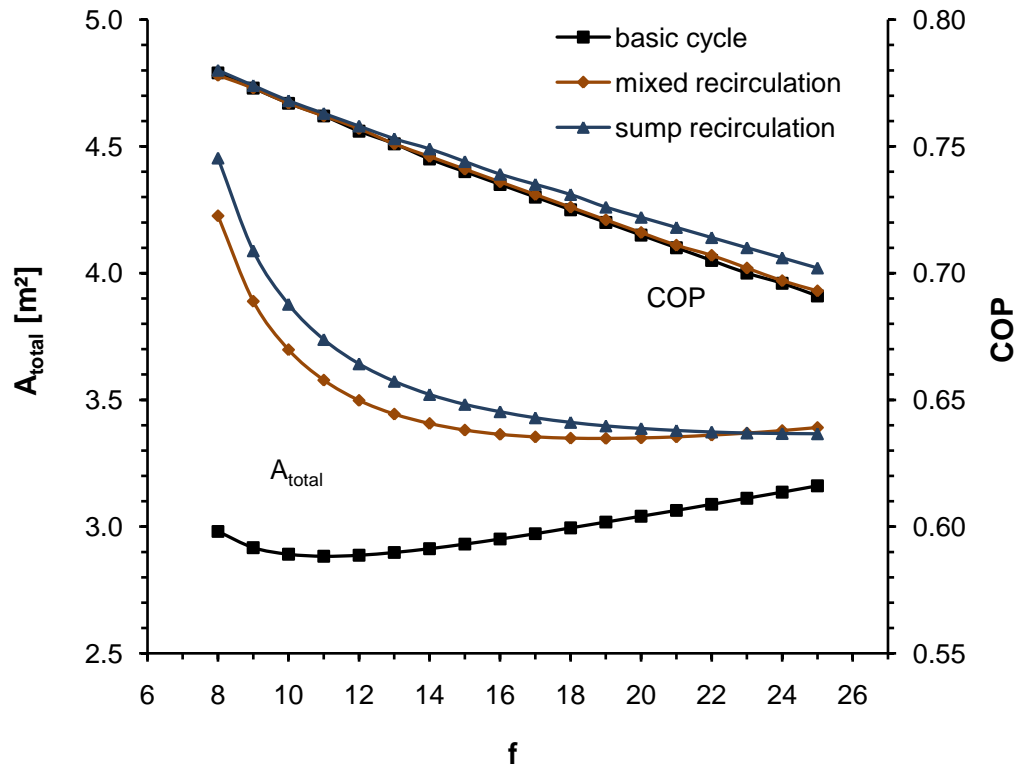
Figure 4.3: Overall area optimized calculation of cycle concepts

coefficients - which are valid for good wetting. As stated in section 4.1.1, good wetting of the plate heat exchanger requires a certain solution mass flow rate per area; some $0.15 \ kg/m^2s$ for the current plate design. Now, figure 4.1 shows that the solution mass flow rate applied per absorber heat exchanger area for the basic cycle is far below the required value of $0.15 \ kg/m^2s$. Thus, wetting of the absorber heat exchanger will be poor. Hence the heat exchanger area will not be large enough to provide the heat and mass transfer rates necessary for the design chilling performance.

Consequently, the result for the basic cycle shown in figure 4.3 may be well valid for bundled tube heat exchangers, but not for a plate heat exchanger type as we intend to use. Now, how can the heat exchanger wetting be enhanced? As elaborated in section 4.1.1, by solution recirculation rather than by increasing f.

For the cycle calculation of the recirculation concepts, we prescribe a specific solution mass flow rate of $0.15 \ kg/m^2s$, thus providing good wetting. Hence, the calculated absorber heat exchanger area is sufficient because it provides enough heat and mass transfer area for the vapor absorption, in contrast to the basic cycle concept without solution recirculation, which does not provide good wetting.

The orange and blue curves in figure 4.3 show the total heat exchanger area and COP for mixed recirculation and sump recirculation at the absorber. Especially for low values of f, both recirculation concepts' A_{total} is significantly larger than the basic cycle's

A_{total}. This is due to the different concentrations of the solution applied on the absorber heat exchanger:

In the basic cycle, poor solution coming from the generator is applied on the absorber heat exchanger. Having a low water concentration, this solution can absorb much vapor. In the cycles with recirculation however, rich solution from the absorber sump is applied on the absorber heat exchanger, either pure or mixed with poor solution coming from the generator. In either case, the applied solution contains much more water than the poor solution. Hence, more solution is necessary to absorb the vapor coming from the evaporator. With the specific mass flow rate (that is, mass flow rate of the applied solution divided by the absorber heat exchanger area) being constant, an increased solution mass flow rate also means an increased absorber heat exchanger area. For f below 23, the cycle with sump recirculation has a somewhat larger total heat exchanger area than the cycle with mixed recirculation. That difference is mainly because of the larger absorber area, see figure 4.4, where the two upper curves depict the absorber heat exchanger area for the two recirculation concepts. The larger absorber area in turn results from the higher water content of the applied solution: The richer solution can absorb less water.
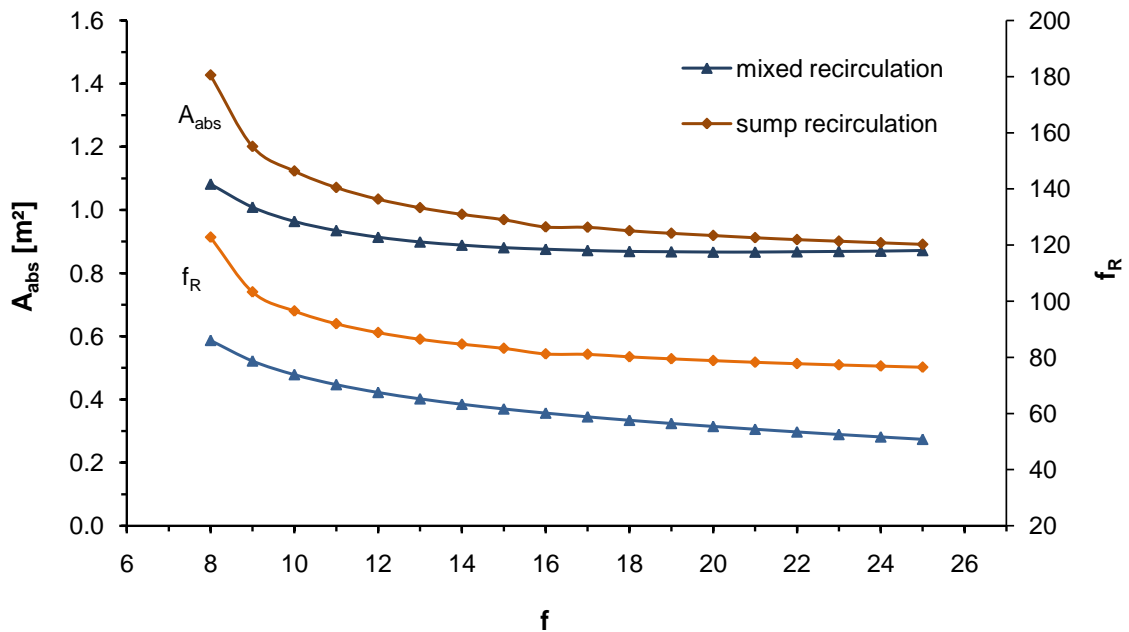

Figure 4.4: Absorber heat exchanger area and recirculation ratio for absorption cycles with solution recirculation at the absorber

Figure 4.4 also depicts the solution recirculation ratio f_R, defined as the ratio of the mass flow rate of the recirculated solution and the refrigerant mass flow rate:

$$f_R = \frac{m_{recirc}}{m_{refr}}. \tag{4}$$

For the sump recirculation concept, only the recirculated solution is applied on the absorber, whereas the poor solution coming from the generator flows into the absorber sump. Hence, the specific mass flow rate, that is, the mass flow rate applied on the absorber per absorber area, is

$$m_{spec,sump} = \frac{m_{recirc}}{A_{abs}}, \tag{5}$$

and the recirculation ratio writes

$$f_{R,sump} = \frac{m_{recirc}}{m_{refr}} = \frac{m_{spec} \cdot A_{abs}}{m_{refr}}. \tag{6}$$

For the mixed recirculation concept however, the poor solution coming from the generator is part of the solution that is applied on the absorber and the specific mass flow rate writes

$$m_{spec} = \frac{m_{recirc} + m_{poor}}{A_{abs}}. \tag{7}$$

With m_{poor} being

$$m_{poor} = m_{rich} - m_{refr} = m_{refr}(f - 1), \tag{8}$$

this term becomes

$$m_{spec} = \frac{m_{recirc} + m_{refr}(f - 1)}{A_{abs}} \tag{9}$$

and solving for m_{recirc} yields

$$m_{recirc} = m_{spec} \cdot A_{abs} - m_{refr}(f - 1), \tag{10}$$

and finally the recirculation ratio for mixed recirculation writes

$$f_{R,mixed} = \frac{m_{recirc}}{m_{refr}} = \frac{m_{spec} \cdot A_{abs}}{m_{refr}} - f + 1. \tag{11}$$

Equations (6) and (11) show that for mixed recirculation, the solution circulation ratio f influences the recirculation ratio f_R considerably more than it does for sump recirculation. $f_{R,sump}$ is only influenced by f via the absorber area, which is a function of f. The equation for $f_{R,mixed}$, however, additionally contains the term -f. That explains the form of the $f_{R,mixed}$ curve in figure 4.4: With the curve for the absorber area approaching a linear shape with increasing f, the term $\frac{m_{spec} \cdot A_{abs}}{m_{refr}}$ virtually becomes constant. Hence, the curve for $f_{R,mixed}$ approaches a linear function with the slope -f. As the slope of $f_{R,sump}$ is larger than f, the two curves diverge. Within the relevant range of f, the difference is moderate, and thus also the additional pump work. Consequently, the higher recirculation mass flow rate of the sump recirculation concept is not a decisive criterion against the concept.

One more look at figure 4.3 shows that for mixed recirculation, the COP is virtually equal to the COP of the basic cycle whereas the sump recirculation cycle's COP is somewhat better for f larger than twelve. However, the differences are relatively small for moderate values of f. And as to area optimization, an increase of f beyond, say, sixteen, has only little effect. For mixed recirculation, A_{total} even begins to rise again at an increase of f beyond eighteen.

What conclusions can we draw from these results? First, solution recirculation is a promising approach to improve wetting of the absorber plate heat exchanger. Second, mixed recirculation and sump recirculation perform similarly. From the heat exchanger area and COP point of view, they are more or less equal. Sump recirculation requires somewhat more pump work for the solution recirculation. Third, there is no absolute design optimum. The design is a compromise between reaching a low heat exchanger area and a good COP. While the heat exchanger area determines the material costs, the weight, and the achievable compactness of an absorption chiller, the COP determines the energy input needed for a certain chilling performance and thus impacts the running costs. A more detailed evaluation of economic and energetic aspects as, for instance, material prices and the necessity to reduce the operating energy consumption is necessary to decide on the best compromise between low heat exchanger area and high COP.

4.2 Equal Heat Exchanger Sizes

In the previous section, we discussed solution recirculation at the absorber as an approach to overcome the poor wetting of the used plate heat exchangers and the bad performance connected with it. Now we will investigate another design approach, one that has little to do with performance enhancement but more with cost reduction: Equal heat exchangers. The question we are going to discuss is: What impact does it have on the overall heat exchanger area and the COP, if (1) the absorber and the evaporator and (2) the absorber and the evaporator, and the generator and the condenser, have pairwise the same size, that is, the same heat exchanger area.

The motivation for this question is: If pairwise equal heat exchangers can be used in the absorption chiller, fewer heat exchangers have to be engineered and fewer heat exchanger variants have to be produced. Moreover, the pairwise equal heat exchangers, could even be made on the same plate. For instance, the absorber and the evaporator on one plate. Production and assembly costs of the main components would reduce notably, as illustrated in section 3.3. Thus, equal heat exchangers are a promising approach to reduce the production costs for the absorption chiller and thus the first cost of the chiller. If the absorption chiller shall have a chance to establish on the market, its final price must not be significantly higher than the final price of compression chillers with comparable capacity.

Now, what impact does it have on the entire absorption chiller if the absorber and the

evaporator heat exchanger are equal? And if additionally the condenser is equal to the generator? Consider figure 4.5, depicting the result of cycle calculations with the same input data as for the previous cycle calculations, but with the modification that (1) the absorber and the evaporator are equal in size ($A_{abs} = A_{evap}$, medium colored curves), and (2) additionally the condenser and the generator are equal in size ($A_{abs} = A_{evap}$ and $A_{gen} = A_{con}$, light colored curves). The dark colored curves are for individually optimized heat exchanger areas, that is, equal to the curves in figure 4.3.
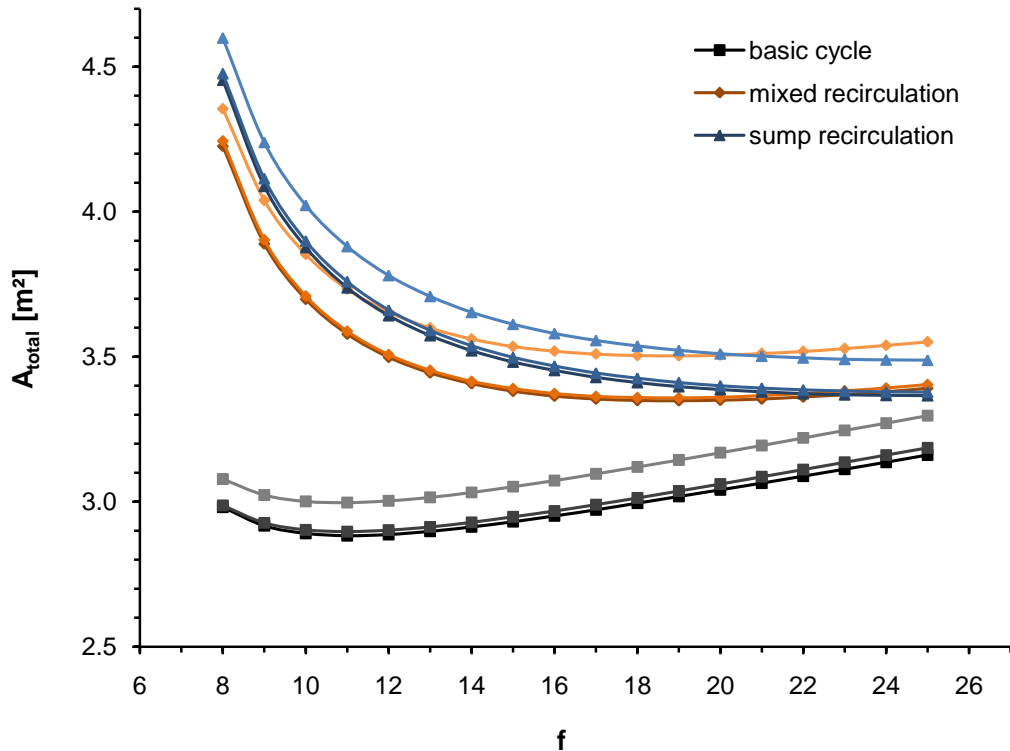

Figure 4.5: Overall heat exchanger area with different cycle designs and area optimization concepts. Dark colored curves: Minimum overall heat exchanger area; individual optimization for every heat exchanger. Medium colored curves: $A_{abs} = A_{evap}$. Light colored curves: $A_{abs} = A_{evap}$ and $A_{gen} = A_{con}$.

The dark and medium colored lines are close together. For mixed recirculation (orange curves), it is even hard to distinguish between them as the medium orange curve is only slightly above the dark orange curve. In other words: Making the heat exchanger areas of absorber and evaporator equal results in a negligible increase of the overall heat exchanger area.

However, the light colored curves are considerably above the dark and medium colored curves. That means, making not only the absorber and evaporator, but also the generator and condenser pairwise equal does increase the overall heat exchanger area compared to an individual optimization of all main component heat exchanger areas. For mixed recirculation, this impact is somewhat stronger than for sump recirculation; the distance

between the light, and the medium and dark colored curve is larger than it is for sump recirculation.

On the one hand, the previous results show that compared to sump recirculation, mixed recirculation results in a somewhat lower overall heat exchanger area and a slightly lower or equal COP. On the other hand, sump recirculation has constructive advantages compared to mixed recirculation. The pump for the rich solution must increase the pressure far enough so that the rich solution can enter the absorber. Depending on how the mixed solution is applied on the absorber heat exchanger, the pressure after the pump may have to be even higher than the internal pressure in the generator. In that case, however, the poor solution coming from the generator will be stopped from flowing to the absorber. Hence, simply connecting the pipes as sketched in figure 4.2(a) does not work. As sump recirculation is easier to carry out and has only slight disadvantages as to COP and heat exchanger area, it is the preferable recirculation concept. So, let us have one more close look on the results of the cycle calculation for the sump recirculation concept, depicted in figure 4.6.
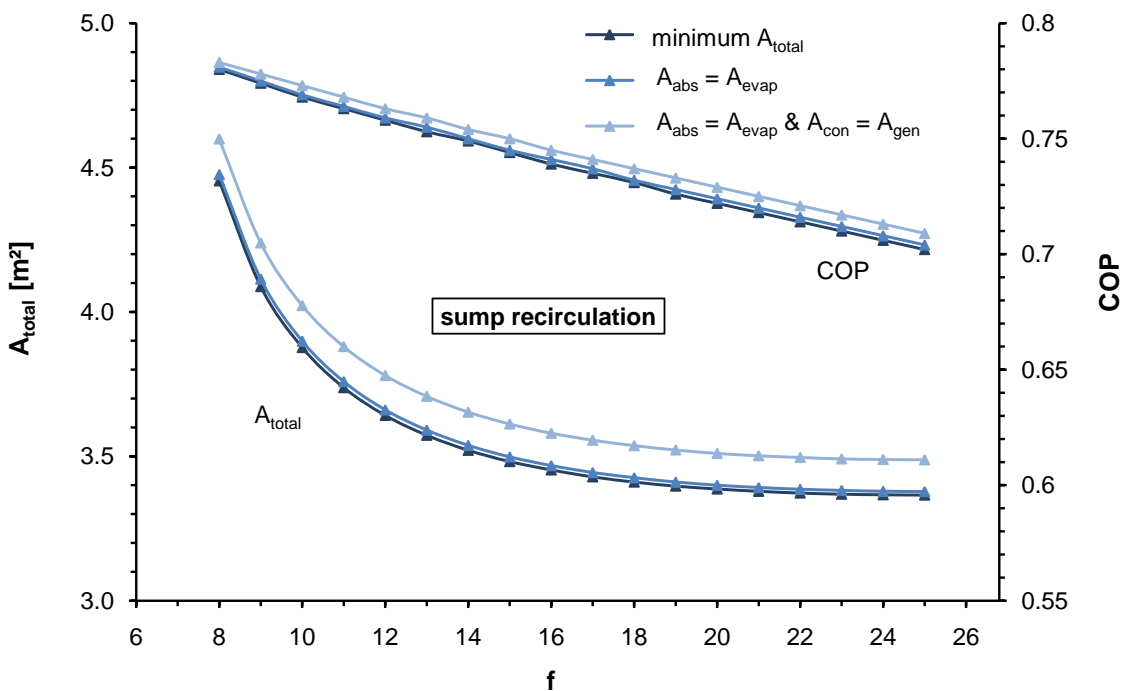
Figure 4.6: Overall heat exchanger area and COP for the sump recirculation concept

Besides the overall heat exchanger area, the diagram also shows the COPs for the different heat exchanger optimization concepts. Making the evaporator and the absorber equal has little effect, both on the area and the COP. Yet, as found above, if also the condenser is equal to the generator, the overall heat exchanger area is considerably larger, which is a disadvantage. As figure 4.6 shows, however, also the COP increases a bit,

which is favorable. The reason for this COP increase is that with larger heat exchangers, lower temperature differences between the fluids are needed to transfer the same amount of heat, and thus the losses are lower and the heat transfer is more efficient. Hence, the driving heat needed for the four kilowatt chilling capacity decreases.

4.3 Pool Generator

After having investigated the effect of recirculation and making the heat exchangers pairwise equal, we will now elaborate whether using a pool generator is promising for our design problem. This sections consists of four subsections. The first subsection presents the concept of and the motivation for using a pool generator, as well as possible constraints. The second subsection briefly states the assumptions for the model of the pool generator. The third subsection contains a calculation estimating the heat transfer coefficient for the flooded plate heat exchanger. Lastly, the fourth subsection presents the results of the calculations for the absorption chiller cycle with sump recirculation and pool generator.

4.3.1 Concept, Motivation and Constraints of a Pool Generator

Pool generator means that the solution is not applied on top of the heat exchanger and then forms a falling film flowing down along the heat exchanger plates, as it works in falling film heat exchangers. Instead, the generator is a pool, partly filled with solution and the generator heat exchanger is partly flooded by the solution [Estiot (2009)].
In the pool, nucleate boiling generates vapor bubbles. Because of the low pressure in the generator - in our case some seventy millibars -, the specific volume of the vapor is very high and thus the solution bubbles intensely. The intense bubbling makes solution splash on the upper part of the heat exchanger - the part that is above the solution surface and that is dry when the solution is in rest. In this way, the entire heat exchanger is wetted with solution.
Now, why use a pool generator, what are its advantages? First, thanks to the intense bubbling, pool boiling provides good wetting without recirculation. Recirculation at the absorber works without an additional pump, because one and the same pump can deliver the recirculated solution and the solution leaving to the generator. At the generator however, the outgoing solution does not have to be pumped because the pressure drop from the generator to the absorber is sufficient to make the solution flow from the generator to the absorber. Hence solution recirculation at the generator requires an additional pump. A pool generator however does not need recirculation and hence not need that additional pump. That saves both pump work and the weight and money for the pump. Moreover, the piping for the recirculated solution can be omitted.
Second, as the pool generator is simply flooded with solution, it does not need any solu-

tion application system. To sum up the first two advantages, pool boiling reduces both weight and costs of the generator - even if the additional solution in the generator sump increases the weight somewhat.

Third, pool boiling promises higher heat transfer rates and thus a smaller heat exchanger area than film boiling. [Estiot (2009)] showed the benefit of operating a generator with a tube bundle heat exchanger in pool boiling mode if the wall superheat is at least thirteen Kelvin. Assumed that pool boiling is as effective in plate heat exchangers, pool boiling allows for reduction of the generator heat exchanger and consequently reduces weight and costs, too.

But does a pool generator really suit the prerequisites for our absorption chiller? Pool boiling requires a larger wall superheat than film boiling. Remember, the planned hot water inlet temperature is only ninety degrees Celsius. And here, the low pressure level in the generator is unfavorable, because the hydrostatic pressure has a strong impact on the local saturation temperature of the solution.

Consider figure 4.7, depicting a sketch of a pool with lithium-bromide solution. The solution has a concentration of fifty-eight percent lithium-bromide, the surface pressure is sixty-five millibar, and the saturation temperature at the surface is some seventy-seven degrees Celsius. Below the surface, however, the saturation temperature of the solution increases fast with increasing depth. In only one centimeter depth, the saturation temperature is above eighty degrees, and in five centimeter depth it already reaches some ninety-five degrees Celsius.
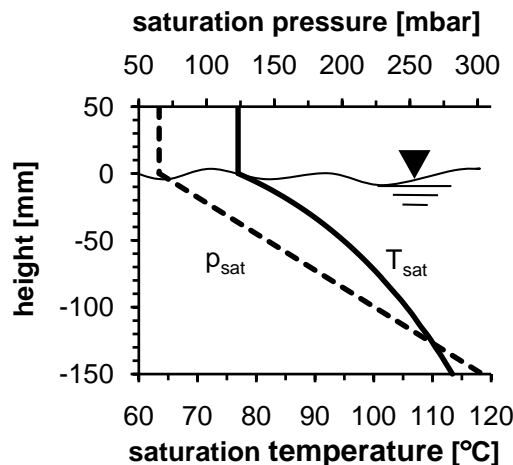
Figure 4.7: Equilibrium temperature of LiBr solution in a pool. The LiBr concentration is 58%, the vapor pressure is 65 mbar.

The Dühring plot, figure 2.3, helps to understand that quick increase of the saturation temperature with increasing depth. The axis for the saturation pressure is logarithmic while the axis for the saturation temperature is linear. Hence, at low pressure levels, pressure differences have a much stronger impact on the saturation temperature than at

high pressure levels. At a fifty-eight percent concentration, the lithium-bromide solution has a density of some 1600 kg/m^3. That means, for every ten millimeters of depth, the hydrostatic pressure in the pool rises by almost 1.6 millibar, which is much compared to the sixty-five millibar surface pressure. Now, another look at the Dühring plot shows why the saturation temperature in the pool rises so quickly.

4.3.2 How to Model a Pool Generator

As elaborated above, the hydrostatic pressure has a notable influence on the local saturation - that is, boiling - temperature. Hence the model for the numerical calculation should take this interrelation into account. To calculate local heat transfer coefficients in a tube bundle pool generator, [Estiot (2009)] used the local saturation temperatures of the solution in the middle of the respective tube.
This discretization can be carried over and be used to model a pool generator with a plate heat exchanger. Figure 4.8 sketches how to carry out the discretization. For the heat exchanger, we assume a height of one hundred millimeters. Half of the heat exchanger is flooded, so the height of the solution to be discretized is fifty millimeters. These heights for the heat exchanger and the solution correspond to those in [Estiot (2009)], for which Estiot found in her experiments that the pool generator performed well. The model discretizes the solution, which is fifty millimeters high, into one hundred layers, so each layer's height dh is a half millimeter. For every layer, the local pressure and the respective saturation temperature are determined, under the assumption that concentration gradients within the pool are negligible.
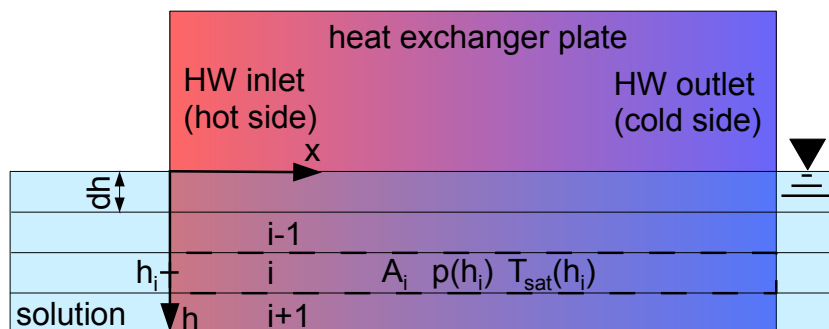
Figure 4.8: Discretization of the flooded part in the pool generator

The saturation temperature of the solution in the pool increases with increasing depth, yet we assume that because of good mixing there is no horizontal temperature gradient on the solution side. But as the flow direction of the hot water (HW) on the other side of the heat exchanger plate is horizontal and water loses heat as it heats the solution, there is a horizontal temperature gradient on the water side. We assume however that the vertical temperature gradient on the water side is negligible because the forced flow

results in good vertical mixing.

Because of the vertical temperature gradient in the pool, the heat transfer rate is a function of the depth. The local logarithmic mean temperature difference is

$$lmtd(h) = \frac{(t_{HW,in} - t_{pool}(h)) - (t_{HW,out} - t_{pool}(h))}{ln\left(\frac{t_{HW,in} - t_{pool}(h)}{t_{HW,out} - t_{pool}(h)}\right)} \tag{12}$$

and rewriting yields

$$lmtd(h) = \frac{t_{HW,in} - t_{HW,out}}{ln\left(\frac{t_{HW,in} - t_{pool}(h)}{t_{HW,out} - t_{pool}(h)}\right)}. \tag{13}$$

Now, the heat transfer rate in the layer i is

$$q_i = A_i \cdot U_i \cdot lmtd(h_i), \tag{14}$$

where A_i is the area of one layer and equal for all layers, and U_i is the overall heat transfer coefficient for h = h_i. Let us assume that, within the small height of the pool, the overall heat transfer coefficient is constant, U_{pool}. Then the heat transfer rate for the flooded part of the generator is the sum of the heat transfer rates of all layers:

$$q_{flooded} = \sum_i q_i = A_i \cdot U_{pool} \cdot \sum_i lmtd(h_i). \tag{15}$$

The flow regime of pool boiling in a plate heat exchanger differs much from that in a horizontal tube bundle. Hence, the overall heat transfer coefficient U_{pool} is not a value measured by [Estiot (2009)] but an estimation based on the findings of [Lee et al. (1991)] and [Kaji et al. (1995)], see section 4.3.3 below.

According to the model, the intense boiling splashes saturated solution from the pool on the upper part of the generator heat exchanger. The solution then forms a falling film, hence the upper half of the generator is calculated as a falling film heat exchanger.

4.3.3 Convective Heat Transfer Coefficient in the Pool

Other than for the falling film heat exchangers, where we could use measured U-values of a tested absorption chiller, little information is available on the heat transfer coefficients of pool generators. [Estiot (2009)] investigated subatmospheric pool boiling of aqueous LiBr-solution for plain and finned horizontal tube bundle heat exchangers, but not for vertically arranged plate heat exchangers as we will model. Also most other publications on subatmospheric pool boiling of aqueous LiBr-solution refer to horizontal tubes, mostly single tubes, or horizontal plates.

In contrast to falling film boiling, buoyancy plays an important role in pool boiling. Buoyancy forces vapor bubbles to move upwards, and that motion substantially rules

the flow regime in the pool and thus the convective heat transfer. The bubble motion however is influenced by the arrangement of the heat exchanger - be it consisting of tubes or of plates -, because the arrangement determines the paths the bubbles can take. For instance, the flows between the tubes of a horizontal tube bundle and a vertical tube bundle differ. Different flows, however, result in different convective heat transfer co-efficients. For example, single vertical tubes reach a higher heat transfer than single horizontal tubes in subatmospheric LiBr-solution [Lee et al. (1991)].

Concludingly, it is advisable to estimate the convective heat transfer coefficient of the pool generator we will model by means of data referring to vertically arranged heat exchangers, because our plate heat exchanger will also be arranged vertically.

[Lee et al. (1991)] and [Kaji et al. (1995)] made experiments with a vertical tube and a vertical plate, respectively, and determined the convective heat transfer coefficient for subatmospheric pool boiling of aqueous lithium-bromide solution. Lee et alii immersed an eleven millimeter diameter and 120 millimeter long cylinder in aqueous LiBr-solution with a 55 percent LiBr mass fraction. They heated the cylinder and determined the heat transfer coefficient in the middle of the cylinder, that is, 60 millimeters below the surface of the solution. They conducted measurements at varying wall superheat and at four different system pressures between 30 and 300 torr, that is, between 40 and 400 millibars. The diagram in figure 4.9 plots the measured convective heat transfer co-efficients at 40, 93 and 200 millibars, for a twelve Kelvin wall superheat - which should be enough for a well-working pool generator [Estiot (2009)].
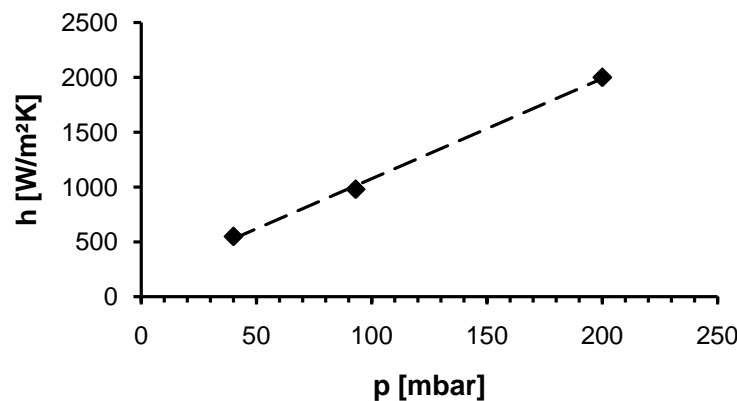
Figure 4.9: Convective heat transfer coefficients of boiling aqueous LiBr solution measured by [Lee et al. (1991)]. ΔT_W = 12K, x_{LiBr} = 55%. Dashed line: linear fit.

A linear fit - the dashed line in the graph - points on a linear correlation between the saturation pressure and the heat transfer coefficient in the range between 40 and 200 millibars. Based on the previous cycle calculation results, we assume a 70 millibar pressure in the generator, a pressure located within the linear range between 40 and 200 millibars. Hence, linear interpolation yields the estimated convective heat transfer

coefficient h_{pool}:

$$\frac{(2000 - 550)W/m^2K}{(200 - 40)mbar} = \frac{h_{pool} - 550W/m^2K}{(70 - 40)mbar} \tag{16}$$

$$h_{pool} = 822 \, \frac{W}{m^2K} \tag{17}$$

Let us compare this value with the results of [Kaji et al. (1995)], who conducted experiments with a heated vertical plate immersed in 55∼58 percent aqueous LiBr-solution. For a twelve Kelvin wall superheat and 240 millibars pressure, they measured a heat transfer coefficient of 760 W/m²K, only a little lower than for a atmospheric pressure, where they measured some 790 W/m²K.

On first sight, the result of Kaji et alii seems to point on lower heat transfer coefficients than those measured by Lee et alii. 760 W/m²K at 240 millibars is considerably lower than the 2000 W/m²K at 200 millibars measured by Lee et alii. Kaji et alii did not measure at pressures lower than 240 millibars but at lower pressures, the heat transfer is worse, so the result suggests that at a 70 millibars pressure, the heat transfer coefficient is considerably lower than the 760 W/m²K at 240 millibars.

However, Kaji et alii's plate was deeper under the solution surface than Lee et alii's tube. Even though their paper does not reveal the exact depth, they measured the heat transfer more than 100 millimeters under the surface. Not either does the paper mention where the system pressure was measured - probably in the vapor atmosphere above the pool, as Lee et alii did, but that is not certain. Another uncertainty in [Kaji et al. (1995)] is the solution concentration. It is between 55 and 58 percent, but the exact concentration is not stated. [Lee et al. (1991)] however found that even small concentration increases result in lower heat transfer. The higher solution concentration in Kaji et alii's experiments is certainly a major reason for the lower heat transfer coefficients compared to Lee et alii's.

Yet another uncertainty is the surface finish. [Lee et al. (1991)] used a precision grinding machine to obtain a smooth heating surface, [Kaji et al. (1995)] used "#2000 emery paper". Neither of the papers however states the actual surface roughness of the heating surface, even though the roughness influences bubble formation and thus the heat transfer.

To sum up, the results in [Kaji et al. (1995)] point on somewhat lower heat transfer coefficients than [Lee et al. (1991)], yet differences in the experiment designs and the elaborated uncertainties make it difficult to compare the results of the two publications one to one. Moreover, Lee et alii measured in the pressure range relevant for our application, while Kaji et alii only measured at 240 millibars and at atmospheric pressure. Hence, Kaji et alii's result does not allow to make a good estimate of the heat transfer coefficient at 70 millibars. Consequently, the data in [Lee et al. (1991)] is more significant and suits better for an estimate, so let us assume that $h_{pool} = 822$ W/m²K, as

calculated with equation (16).

The U-value, or overall heat transfer coefficient, respectively, of the flooded part of the heat exchanger writes

$$U_{pool} = \left(\frac{1}{h_{pool}} + \frac{s}{k} + \frac{1}{h_c} \right)^{-1},$$

(18)

where s and k are the thickness and the conductivity of the stainless steel heat exchanger plate, respectively, and h_c is the convective heat transfer coefficient on the cooling water side. The plate is $s = 0.4$ millimeters thick - see also section 5.4 - and has a conductivity $k = 15$ W/m·K. For h_c, let us assume 4000 W/m²K - see also section 5.5.1. Applying these values yields the U-value

$$U_{pool} = \left(\frac{1}{822 \, \frac{W}{m^2 K}} + \frac{4 \cdot 10^{-4} \, m}{15 \, \frac{W}{m \, K}} + \frac{1}{4000 \, \frac{W}{m^2 K}} \right)^{-1} = 670 \, \frac{W}{m^2 K}.$$

(19)

4.3.4 Results of the Pool Generator Calculations

As mentioned above, the calculation model considers both a pool generator and solution recirculation according to the sump recirculation design - see section 4.1.2 - at the absorber. The calculations do not converge when using the planned external temperatures of 10/15 degrees Celsius for the chilled water, 30/38 degrees Celsius for the cooling water and 80/90 degrees Celsius for the hot water. That indicates that the cycle does not work with the planned external temperatures.
Reducing the cooling water temperature level by three Kelvin yields the results depicted in figure 4.10. The plot depicts the total heat exchanger area over the hot water inlet temperature for two cycle calculations, one with the solution circulation ratio f = 15, and one with f = 20. With increasing hot water inlet temperature, the needed heat exchanger area decreases. The reason for this is that for higher wall superheat, the area needed to transfer the required heat is lower.

The actual finding of the calculations however is: In spite of the reduced cooling water temperature level, the planned hot water temperature level of 80/90 degrees Celsius is not sufficient. For f = 15, the calculation does not converge for hot water inlet temperatures below 94.5 degrees Celsius. For f = 20, the minimum hot water inlet temperature is 93 degrees Celsius. Another approach would be to increase the chilled water temperature to, for instance, 15/18 degrees Celsius.

To conclude, with the planned external temperatures, the absorption chiller cannot have a pool generator. Using a pool generator in spite requires to adjust the external temperatures. That, however, results in drawbacks:
Increasing the hot water inlet temperature means that reject heat from combined heat
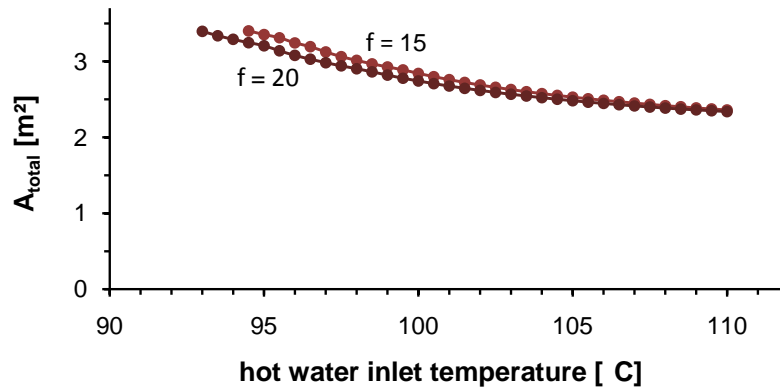
Figure 4.10: A$_{total}$ over the hot water inlet temperature for an absorption chiller with pool generator and absorber sump recirculation. The hot water outlet temperature is ten Kelvin below the respective inlet temperature. The cooling water temperatures are 27/35 degrees Celsius and the chilled water temperatures are 10/15 degrees Celsius.

and power plants may be on a too low temperature level and hence no longer be suitable. Moreover, it complicates the use of solar panels to produce the hot water. Even though solar panels can heat water to temperatures above 90 degrees Celsius, it is not favorable: For flat plate collectors, losses increase and consequently a larger collector area is necessary, which increases the first cost. Evacuated tube collectors have lower temperature-dependent losses and are therefore more suitable for higher temperatures. Nevertheless, they cost significantly more than flat plate collectors.

A cooling water temperature level below 30/38 degrees Celsius requires a wet cooling tower. In contrast, depending on the local maximum outdoor temperatures, 30/38 degrees cooling water can also be realized with a dry cooling tower, which is less costly than a wet cooling tower [Natzer et al. (2010)]. If the local climate does not allow to use a dry cooling tower, however, higher cooling water temperatures still require a smaller cooling tower, which reduces the application's first cost. Hence, keeping the cooling water temperature level at 30/38 degrees Celsius would be favorable.

Increasing the chilled water temperature to, for instance, 15/18 degrees Celsius has drawbacks, too. That temperature level is too high to dry the chilled air. Thus, the chilled air becomes humid and that means a reduced comfort for the persons present in the respective air conditioned room. Nevertheless, 15/18 degrees chilled water can provide enough chill for radiant cooling, for instance with ceiling panels.

Note that the pool generator calculation is based on an overall heat transfer coefficient in the pool of U_{pool} = 550 W/m^{2}K, a somewhat more conservative estimation than the above derived 670 W/m^{2}K. When the present work was due to be finished, the remaining time was not sufficient to recalculate the cycle with the new U-value. Hence, the calculation underestimates the heat transfer in the flooded part of the generator and thus overestimates the required heat exchanger area. Qualitatively, however, that error does

not impair the validity of the following conclusion:

As becomes obvious, any adoption of the external temperatures has drawbacks. But to realize the absorption chiller with a pool generator, at least one external temperature level has to be adopted. Hence, a pool generator requires a compromise, weighing the different options. Alternatively, the generator could still operate as a falling film heat exchanger.

5 CFD-based Heat Exchanger Design

This chapter aims at the improvement of a plate heat exchanger that was designed as a main component heat exchanger for absorption chillers but performs poorly. The first section gives a brief description of the current heat exchanger design and the reasons for its poor performance, and lists three design goals to improve the heat exchanger. The second section states three design changes to attain the design goals identified in the first section. The third section briefly explains why CFD (Computational Fluid Dynamics) is used as design tool and the fourth section introduces the five heat exchanger designs which are compared and evaluated in the last section of the chapter.

5.1 Design Goals for the New Heat Exchanger

[Behr (2006)] and [Hulin (2008)] investigated the plate heat exchanger depicted in figure 5.1. The heat exchanger had been developed for the use in an absorption chiller. When tested as a falling film absorber, however, the heat exchanger performed worse than expected.

Figure 5.1: The plate heat exchanger investigated by Hulin and Behr

Behr conducted wetting tests and found that wetting on the vapor side of the heat exchanger was poor. Good wetting however is crucial for a falling film absorber to perform well. Hence, Behr concluded that bad wetting is the major reason for the absorber's poor performance. Behr also calculated the heat transfer coefficient on the cooling water side and found that it cannot be the limiting factor of the absorber performance. Hulin confirmed Behr's conclusion. He found that the flow on the water side is well distributed and that the heat transfer on the water side is good: At a mass flow

rate as low as 0.006 kilogram water per second through one plate package[8], Hulin found a value of 3000 W/m^{2}K for the convective heat transfer coefficient on the water side. As good wetting is necessary for a good absorber performance and the current heat exchanger wets poorly, the design of an improved absorber has to aim at improved wetting on the solution side.

Besides wetting, the vapor pressure loss is an important aspect of the absorber design. The absorber will operate at a pressure level of about ten millibars. At such a low pressure level, even a small pressure loss is adverse for the chiller performance. Consider the Dühring-plot in figure 5.2. The saturation pressure on the right vertical axis is given on a logarithmic scale while the horizontal axis for the solution saturation temperature is given on a linear scale. Hence, even small pressure differences at low pressure levels have a considerable impact on the solution saturation temperature.
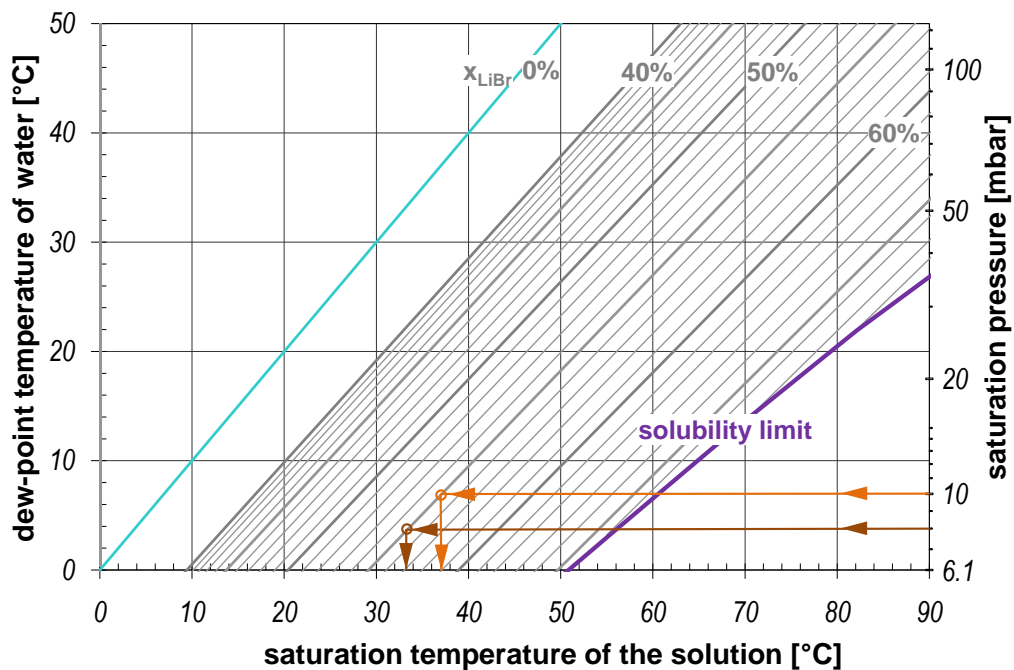

Figure 5.2: Dühring-plot with two different equilibrium states at x = 55%

Consider the following example for which the respective values are sketched in the Dühring-plot, figure 5.2: In the absorber vessel of a lithium bromide absorption chiller, the pressure is ten millibars and the concentration of the lithium bromide solution is fifty-five percent. On its way from the edge to the center of the heat exchanger, the vapor loses two millibars. That is, the pressure at the center of the heat exchanger is only eight millibars. So, at the edge of the heat exchanger, where the pressure is ten millibars, the saturation temperature of the solution is 37 degrees Celsius. In the center

---

[8]A plate package consisting of two heat exchanger plates.

however, where the pressure is eight millibars, the saturation temperature of the solution is only slightly above 33 degrees Celsius, that is, almost four degrees lower than at the edge. Consequently, the driving temperature difference, that is, the temperature difference between the saturated solution on the one side and the cooling water on the other side, is considerably lower in the center. As the heat flux is a linear function of the driving temperature difference, it decreases from the edge of the heat exchanger to the center, in the same extent as the temperature difference. The lower heat flux however reduces the cooling agent absorption rate, because less absorption enthalpy can be cooled by the heat exchanger. As a result, the chilling performance decreases. Similarly, pressure loss in the evaporator causes an increased boiling temperature of the cooling agent. Consequently, the vapor pressure loss in the heat exchanger should be low.

[Behr (2006)] estimated the vapor pressure loss for the current heat exchanger design in a CFD simulation and found that it is reasonable. Behr's model however does neither consider absorption in the vapor channels nor the solution flow and wetting on the plates. It considers a constant vapor mass flow rate in the channels. Consequently, the value of Behr's simulation is limited; it can be seen as a rough estimate. Tests at the Bavarian Center for Applied Energy Research, however, showed that the vapor pressure loss in the current absorber does not limit the performance of the absorption chiller.[9] Insofar, the tests confirm Behr's results.

Admittedly, the results of both the tests and Behr's simulations are strongly qualitative, yet they indicate that the poor performance of the current heat exchanger is not caused by excessive vapor pressure loss. Nevertheless, even though bad wetting is the main problem to be solved, vapor pressure loss should play a role in the design of the new heat exchanger. To avoid a poor chiller performance because of high vapor pressure losses in the heat exchangers, the vapor pressure loss in the new heat exchanger should not be significantly higher than in the current one.

A third aspect to be considered in the design of the new heat exchanger is the pressure loss on the water side. In laminar flows, pressure loss is low; and so is the convective heat transfer. To achieve good convective heat transfer between the fluid and the walls, turbulent flow is by far better than laminar flow. Thus many technical applications, and particularly heat exchangers, require turbulent flow. Yet turbulent flow has a drawback: It causes significantly more pressure loss than laminar flow. Although increased pressure loss on the external side of the heat exchanger, for example in the water cooling the absorber, does not directly affect the thermodynamic cycle on the internal side, it increases the pump work to pump the water through the heat exchanger. And increased pump work results in a lower overall efficiency of the absorption chiller. Thus, the pressure loss on the water side of the new heat exchanger should not be excessive. It should keep below, say, two hundred millibars.

---

[9]The results of the tests were not published. They are in-house knowledge of the institute.

To conclude, the new design for the absorber plate heat exchanger shall provide

- better wetting on the solution side and have

- a reasonable vapor pressure loss and

- a water pressure loss below two hundred millibars.

5.2 Modification of the Heat Exchanger Design

Now, the goal is to make suggestions for changes in the heat exchanger design, so that the new design meets the above listed criteria better wetting, reasonable vapor pressure loss, and water pressure loss below two hundred millibars.

Consider the current plate design *hb*,[10] sketched in figure 5.3. The distance between the water channels is 8.5 millimeters, making the vapor channels rather wide. The intention for wide vapor channels was to increase the cross section for the vapor flow, thus reducing the vapor pressure loss. However, the area between the water channels is rather large and plain and hence not a good surface to be wetted by solution. Moreover, the distances for heat conduction are rather long: Heat absorbed in the middle of the vapor channels is more than four millimeters away from the heat sink, that is, the nearest water channel. To get there, the heat has to be conducted along the plate which only has a 0.4-millimeter section.
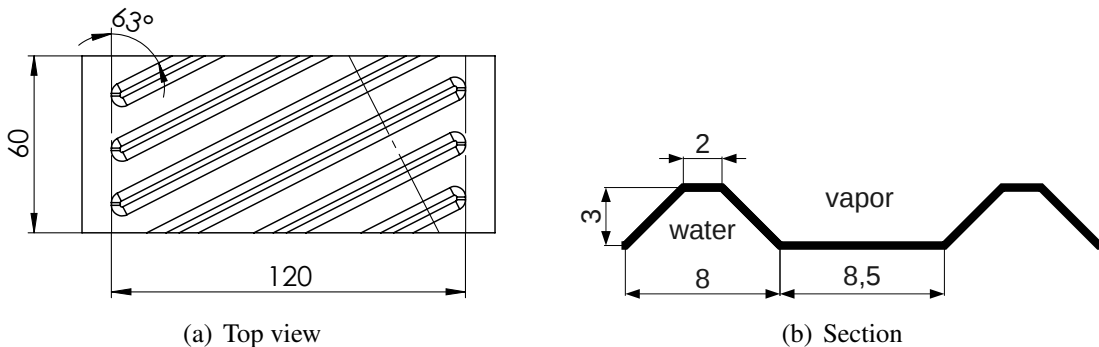

(a) Top view   (b) Section

Figure 5.3: Heat exchanger plate *hb*. In the top view (a), the inclined dot-dashed line in the right part of the heat exchanger is perpendicular to the channels and shows the direction of the section sketch (b). The plate is 0.4 millimeters thick.

In total, the large distance and the thin plate cause a notable thermal resistance and hence notable heat conduction losses. Contrastingly, in a tube bundle heat exchanger, absorption heat only has to be conducted directly through the tube wall, but not along the material. Hence the tube bundle heat exchanger has a significantly shorter heat conduction distance than the current plate heat exchanger. Thus, the thermal resistance

---

[10]The letters *h* and *b* indicate that this is the heat exchanger design investigated by [Hulin (2008)] and [Behr (2006)], see also section 5.4.

and hence the heat conduction losses in the plate heat exchanger are higher than in the tube bundle heat exchanger. Reducing the channel distance improves the plate heat exchanger both as to heat conduction losses and as to surface wetting. In order to keep the increase of vapor pressure loss moderate, we choose to reduce the channel distance to seven millimeters.

Now, the idea to improve wetting on the solution side is to create some kind of substructure between the water channels: water channels, smaller than the existing *main channels*. Let us call these smaller channels *subchannels*. See for example figure 5.4, depicting a plate with two subchannels per main channel. The subchannels divide the planar surface between two adjacent main channels into several smaller surfaces and force the solution flow to change its direction. Presumably, this diversification of the surface on the vapor side improves wetting.

Yet, subchannels have further advantages: First, they increase the plate's surface area. An increased surface area means better heat exchange; more heat can be exchanged per plate (because $Q = U \cdot A \cdot lmtd$). In other words, the heat exchanger becomes more compact because it needs fewer plates to exchange the required amount of heat. The increased surface area is a complement to the improved wetting, the latter resulting in a more efficient use of the available heat exchanger surface area.

Another advantage: Subchannels reduce the heat conduction losses. The cooling water flows not only in the main channels, but also in the subchannels. Consequently, the heat from absorption on or near the subchannels does not have to be conducted as far as to the next main channel but only to the subchannel. As a result, the average distance for heat conduction from the solution to the cooling water decreases and so do the heat conduction losses; the efficiency of the heat exchanger increases.

A drawback of subchannels is, however, that the subchannels reduce the cross section of the vapor channels; and so does the lower distance between the main channels. Hence the vapor pressure loss increases. As mentioned above, not the vapor pressure loss but bad wetting is supposed to be the cause for the current heat exchanger's poor performance. Certainly subchannels and narrower vapor channels increase the vapor pressure loss. We assume, however, that the positive impact of improved wetting and lower heat conduction losses by far outweighs increased vapor pressure losses. This assumption still is to be verified by, for instance, tests of a prototype or simulations. The present work, however, cannot cover that verification.

Moreover, two further design changes can reduce the vapor pressure loss: First, a smaller plate width and second, a larger channel angle. The channel angle is the angle between the channel axis and the side edge of the plate. Both a smaller plate width and a larger channel angle reduce the distance that the vapor has to cover from the edge to the center of the absorber heat exchanger. As to wetting, a smaller channel angle is better than a larger, as [Behr (2006)] found in his wetting experiments. Nevertheless, a moderate increase of the channel angle will be considered.

To sum up, we consider the following changes of the heat exchanger plate design:

- creation of smaller subchannels between the existing channels,

- reduction of the heat exchanger's width, and

- increase of the channel angle.

5.3 CFD-Simulation as Evaluation Tool

In the previous subsections, we discussed the current design of the plate heat exchanger and suggestions to improve the heat exchanger's performance. To get a more detailed idea of the positive or negative effects of the suggestions for an improved heat exchanger design, we need to quantify the effects of the design parameters in question. Therefore, we create a number of plate designs in which one or more of the suggested design changes are implemented, see section 5.4. Comparing the different designs then allows to more accurately evaluate the impact of the different changes. The criteria in that comparison are the heat transfer and the resulting capacity per volume, and the pressure loss on the water side.

For conventional plate heat exchangers, that is, intermating and chevron corrugated plate heat exchangers with a uniform channel size and uniform channel distances, literature offers correlations to calculate the pressure loss and the heat transfer coefficient.[11] Thus, engineers can estimate the performance of a new heat exchanger design quite comfortably. In our case however, the mentioned correlations are not or only partly valid. As [Hulin (2008)] did, we could with some approximations use the existing correlations for our designs without subchannels. The designs with subchannels however are certainly too different from the conventional designs and the respective correlations are not valid for them. Consequently, we do not consider this approach.

Instead, we use Computational Fluid Dynamics (CFD).[12] After designing the heat exchanger plates with the commercial CAD program SolidWorks[13], we analyze them with Flow Simulation, the CFD application within SolidWorks. Flow Simulation can calculate a great variety of flow problems. The user has to define the computational domain and the boundary conditions, can configure a number of settings like mesh generation or convergence criteria, and Flow Simulation then calculates the flow and the specified data like, for instance, pressure, temperature or velocity. As in other CFD applications, the post-processing of Flow Simulation also allows to visualize all calculated characteristics of the simulated flow problem in a number of ways.

---

[11] See for instance [Martin (2006)].
[12] For more detailed information on CFD, see for instance [Versteeg & Malalasekera (1995)].
[13] The used version is SolidWorks 2010.

5.4 Investigated Heat Exchanger Designs

This section presents the above mentioned plate designs that we simulate in order to evaluate the impact of the different design changes suggested in section 5.2. For all designs, a pair of the respective heat exchanger plates is assembled, so that the water side is between the plates. Yet, the simulations do not calculate the entire plate pairs. See for example figure 5.4, showing the isometric view of a simulated plate pair assembly. On both the top and the bottom side, the plates are canted. Thus, only a part of the plates is left; the actual inlet and outlet openings and the distribution and collecting systems for the fluids are cut away.
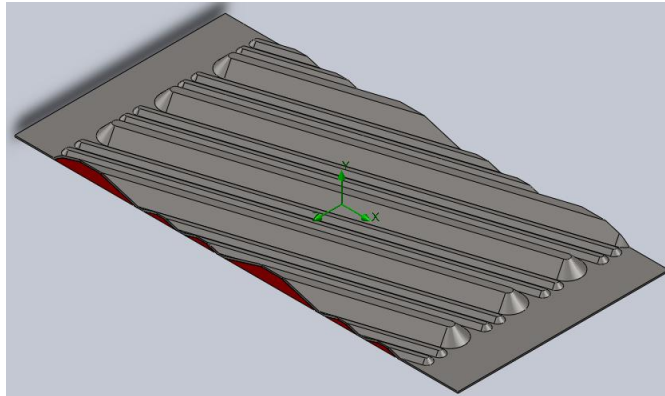

Figure 5.4: Isometric view of the simulated *2sub* plate package

Why not simulate an entire plate package? First, a smaller computational domain allows more accurate results with the given, limited computing power. The mesh for the calculation can be refined to better resolve the turbulent flow and in spite of the refined mesh, the computing time is reasonable. Second, this study focusses on the pattern of the heat exchanger plates, that is, the channel distance, the channel angle and the presence of subchannels. The inlet and outlet region and the adjacent distribution and collecting areas are only small compared to the rest of the plates. Hence, they only cause a relatively small part of the pressure loss, as a prestudy confirmed. And moreover, the distribution and collecting systems of the plates will be redesigned later anyway.[14] Consequently considering the current ones in this study without comparing them with others makes only limited sense - especially as it would also require to coarsen the computational mesh because of the limited computing power at our disposal and hence lead to less accurate results. In short, this CFD study aims at an improved channel structure and thus the simulations focus on the respective part of the plates.

Back to figure 5.4. The water flows through the plate assembly in negative z-direction. Note the red faces in the front. They mark the inlet boundaries of the water. Here, the water enters the plate assembly, flows through the channel pattern and exits at the outlet

---

[14]For reasons of time, the redesign of the inlet and outlet systems cannot be covered within this thesis.

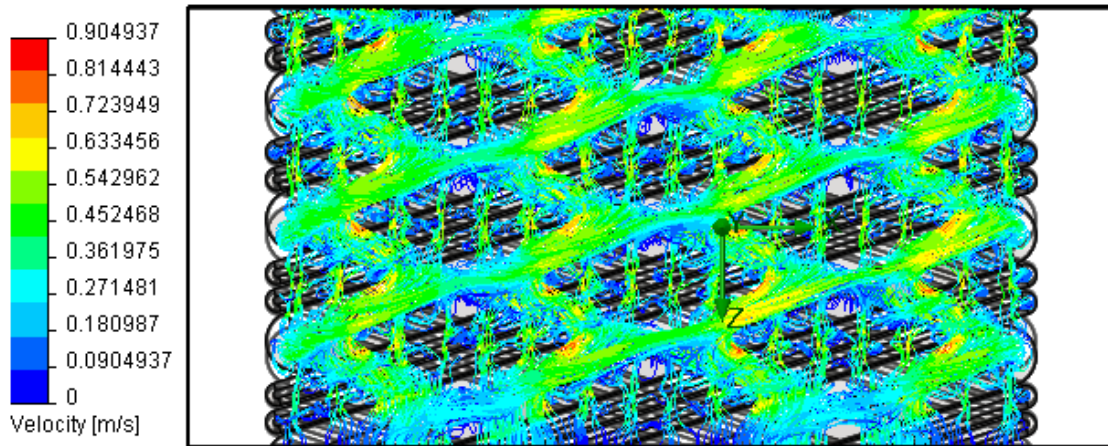boundaries on the back. Figure 5.5 gives an idea of what the flow through the plate assembly looks like.

Figure 5.5: Flow trajectory plot of the *2sub* plate package

The following paragraphs briefly describe the main characteristics of the simulated heat exchanger plates, which are listed in table 5.1. Note that the plate geometries serve to compare the impact of different design features based on the result of the CFD simulations. They are, however, not intended as ready-to-manufacture designs. In fact, minor changes may be necessary before a heat exchanger design can be manufactured.

hb

The letters *h* and *b*, the initial letters of the names *Hulin* and *Behr* indicate that the first plate design to be simulated is the design that was investigated by [Hulin (2008)] and [Behr (2006)]. Figure 5.3 shows the plate. The channels are eight millimeters wide and three millimeters high. The channel angle is 63 degrees, the channel distance is 8.5 millimeters, and the heat exchanger width (that is, the horizontal dimension of the channels, not the distance between the side edges of the plates) is 120 millimeters.

nosub63

The second plate design is depicted in figure 5.6. The term *nosub* in the name indicates that the plate does not have any subchannels. As for the *hb*-design, the channel angle is 63 degrees, indicated by the number *63* in the name. Yet, compared to the *hb*-design the channel distance is reduced from 8.5 to seven millimeters, and the heat exchanger width from 120 to 106 millimeters.

Note: The heat exchanger width of the following designs is not 106, but 100 millimeters. However, those designs have another channel angle, 72.2 degrees. For a 72.2

degrees channel angle and a seven millimeters channel distance, 100 millimeters is an appropriate width, because then, the channels meet at their respective ends and there is no dead range (region with no or very low flow velocity). The channel ends do not meet at 100 millimeters distance, however, if the channel angle is 63 degrees, and the channel distance is kept at seven millimeters. Then, there is no or little flow at the channel ends; the channel ends are a dead range. In dead ranges, the heat exchange is poor and thus dead ranges are to be avoided. So, the width of the *nosub63*-design is not 100 but 106 millimeters.
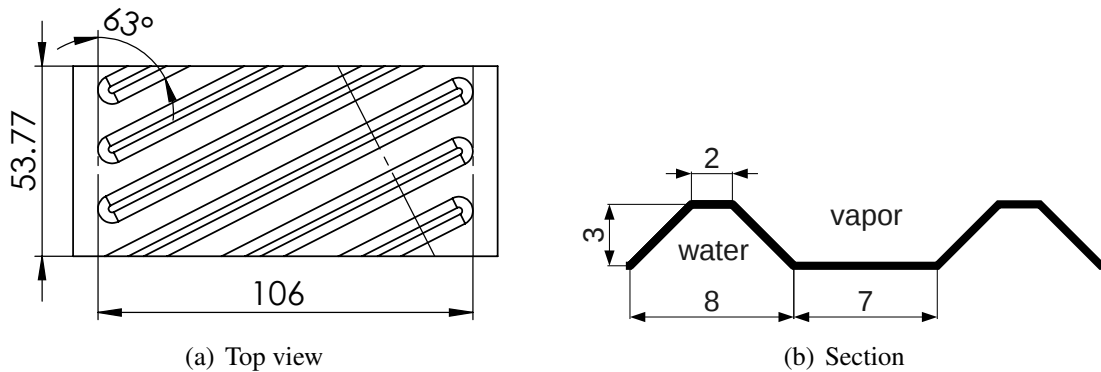

(a) Top view

(b) Section

Figure 5.6: Heat exchanger plate *nosub63*. In the top view (a), the inclined dot-dashed line in the right part of the heat exchanger is perpendicular to the channels and shows the direction of the section sketch (b). The plate is 0.4 millimeters thick.

nosub

The *nosub*-design is depicted in figure 5.7. The name *nosub* indicates that the plate does not have any subchannels. The channel angle is, compared to the previous designs, which had a 63 degrees channel angle, increased to 72.2 degrees. The heat exchanger width is reduced to 100 millimeters, the channel distance is kept at seven millimeters.

1sub

The *1sub*-design is shown in figure 5.8. It has one subchannel centered between two adjacent main channels, which is indicated by the name *1sub*. The subchannel's width is three millimeters, its height one millimeter.

2sub

The last design to be simulated is the *2sub* design, depicted in figure 5.9. The name *2sub* indicates that there is a pair of equal subchannels located between two adjacent main channels. The subchannels have the same size as those in the *1sub*-design, that is, three millimeters width and one millimeter height.
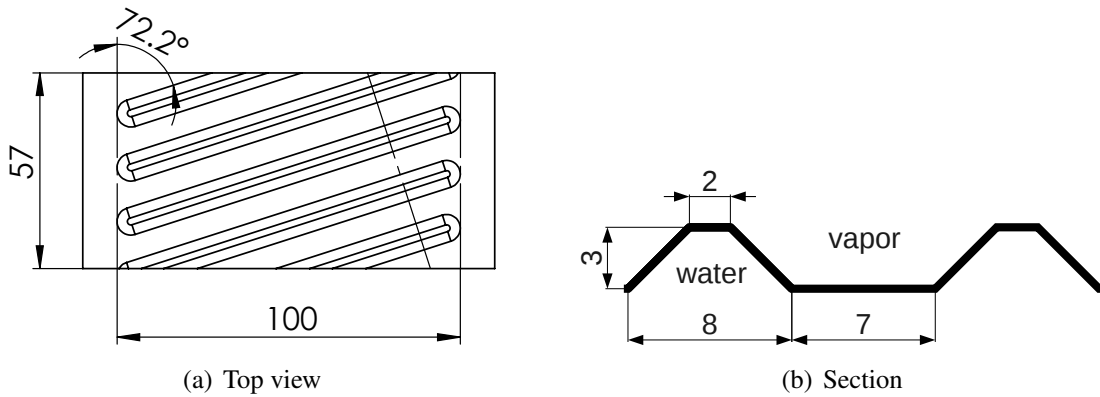
(a) Top view

(b) Section

Figure 5.7: Heat exchanger plate *nosub*. In the top view (a), the inclined dot-dashed line in the right part of the heat exchanger is perpendicular to the channels and shows the direction of the section sketch (b). The plate is 0.4 millimeters thick.

(a) Top view

(b) Section

Figure 5.8: Heat exchanger plate *1sub*. In the top view (a), the inclined dot-dashed line in the right part of the heat exchanger is perpendicular to the channels and shows the direction of the section sketch (b). The plate is 0.4 millimeters thick.
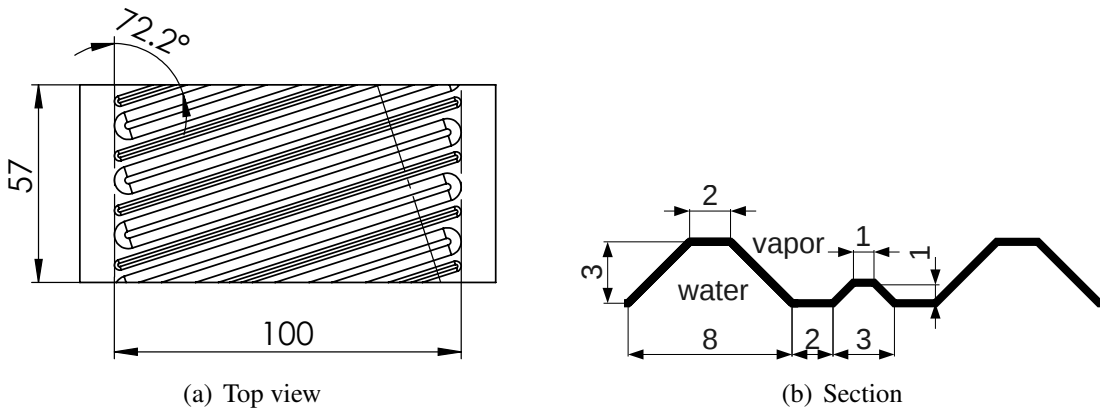

(a) Top view

(b) Section

Figure 5.9: Heat exchanger plate *2sub*. In the top view (a), the inclined dot-dashed line in the right part of the heat exchanger is perpendicular to the channels and shows the direction of the section sketch (b). The plate is 0.4 millimeters thick.
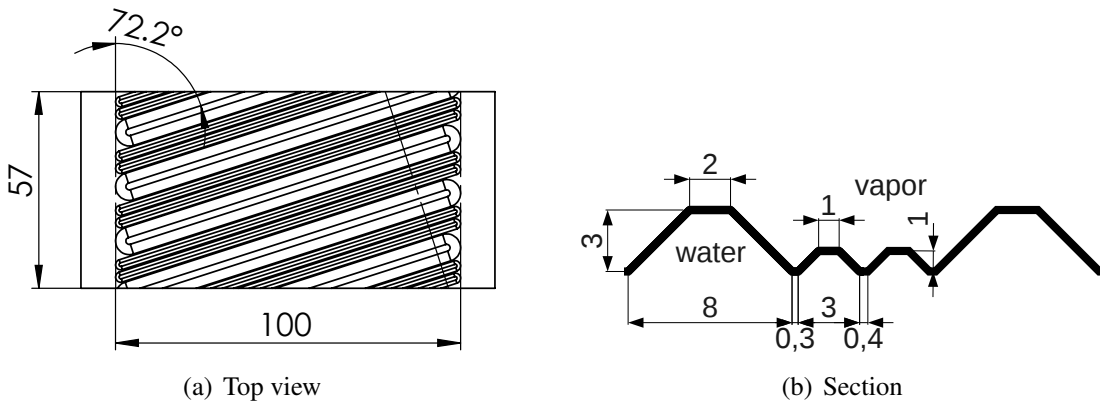
Table 5.1: Main characteristics of the simulated heat exchanger plates. For all plates, the water channels are 8 mm wide and 3 mm deep; the subchannels are 3 mm wide and 1 mm deep.

	hb	nosub63	nosub	1sub	2sub
channel angle [degrees]	63	63	72.2	72.2	72.2
width [mm]	120	106	100	100	100
channel distance [mm]	8.5	7	7	(7)	(7)
subchannels	-	-	-	1	2

5.5 CFD-Simulation

The CFD-based comparison of the different heat exchanger plate designs consists of two steps. First we need to find the required water mass flow rate. Then we simulate all heat exchanger plates at the water mass flow rate determined in the first step. For all the following simulations, the water has a three bars inlet pressure.

5.5.1 Determination of the Water Mass Flow Rate

Before simulating and comparing the different heat exchanger designs, we need to know how much water will be flowing through the heat exchanger. Let us assume that the heat exchanger operates as an absorber and that the absorber transfers $Q = 5000W$ heat at a heat exchanger area of $A = 2$ m^2 and a temperature spread on the cooling water side of $\Delta t_c = 4.4$ Kelvin. The heat exchanger's overall heat transfer coefficient U is 1.0 kW/(m$^2 \cdot$ K). Furthermore let us assume that one heat exchanger plate package, consisting of two plates, has an area of $A_{package} = 0.06$ m^2. Hence, the absorber heat exchanger consists of

$$n = \frac{A}{A_{package}} = 33 \tag{20}$$

plate packages. To sufficiently cool the absorption process on the vapor side, the cooling water flowing through one plate package has to provide a heat capacity rate of at least

$$C_{c,min} = \frac{Q}{n} = 152 \; W. \tag{21}$$

That corresponds to a minimum cooling water mass flow rate of

$$m_{c,min} = \frac{C_{c,min}}{c_{p,water} \cdot \Delta t_c} = 0.0083 \; kg/s \tag{22}$$

flowing through every plate package, with the specific heat of water $c_{p,water}$ = 4.18 kJ/(kg·K).

But $m_{c,min}$ is only the theoretical minimum cooling water mass flow rate necessary to provide the cooling capacity for one plate package. It is based on the assumption of a constant U-value. The U-value, however, is a function of the convective heat transfer coefficients h_f and h_c on the film side and on the cooling water side, respectively:

$$\frac{1}{U} = \frac{1}{h_f} + \frac{s}{k} + \frac{1}{h_c}, \tag{23}$$

where s and k are the thickness and thermal conductivity of the heat exchanger plate. h_c, however, depends on the flow velocity and hence on the mass flow rate of the cooling water. Consequently, also the cooling water mass flow rate and the U-value are interdependent.

Using a 0.4 mm stainless steel plate, we can write s = 0.4 mm and k = 15 W/(m·K). Furthermore we assume that h_f = 1000 W/(m^{2}K). For these values, the plot in figure 5.10 shows U as a function of h_c. At low h_c, U increases quickly. Gradually, the limiting influence of h_c decreases and h_f becomes the limiting factor for U. For a very large h_c, U approaches asymptotically the value of $U_{h_c\infty}$

$$U_{h_c\infty} = \lim_{h_c \to \infty} U = \lim_{h_c \to \infty} \left(\frac{1}{h_f} + \frac{s}{k} + \frac{1}{h_c} \right)^{-1} = \left(\frac{1}{h_f} + \frac{s}{k} \right)^{-1}, \tag{24}$$

and applying the values for the variables yields

$$U_{h_c\infty} = \left(\frac{1}{1000} + \frac{4 \cdot 10^{-4}}{15} \right)^{-1} = 974 \, \frac{W}{m^2 K} \tag{25}$$

That case however requires very high mass flow rates and is therefore rather academic. Let us aim at a convective heat transfer coefficient on the water side, h_c, of 4000 W/m^{2}K or more in order not to limit U too much.

And here we come back to the cooling water mass flow rate, m_c. It determines the water's flow velocity which in turn has a major impact on the convective heat transfer coefficient h_c. Figure 5.11 depicts the results of a prestudy with the plate designs *nosub*, *1sub* and *2sub* and with the mass flow rates 0.01, 0.02 and 0.03 kg/s. The resulting convective heat transfer coefficients are plotted in diagram 5.11(a). At a mass flow rate of 0.01 kg/s, the convective heat transfer coefficient h_c is below 3000 W/m^{2}K for all three plate designs. At the double mass flow rate, 0.02 kg/s, the *nosub* and the *1sub* design have an h_c of some 4000 W/m^{2}K, while the *2sub* design comes somewhat below. A further increase of the mass flow rate to 0.03 kg/s results in all three designs having an h_c above the defined minimum of 4000 W/m^{2}K. As to the heat transfer aspect, 0.03 is the appropriate mass flow rate.

Another aspect to consider however is the pressure loss. High pressure loss in the heat
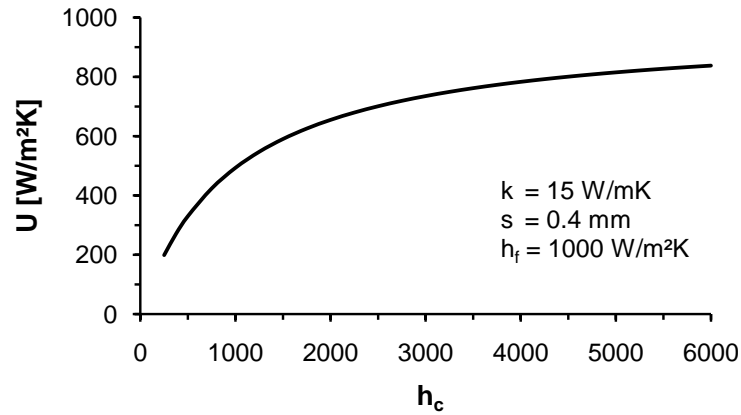
Figure 5.10: The overall heat transfer coefficient U as a function of the convective heat transfer coefficient on the water side

exchanger requires much pump work and thus decreases the overall efficiency of the absorption chiller. Hence, we choose to aim at a pressure loss below 200 millibars. Assuming a plate length of 300 millimeters, the plate designs have the pressure losses plotted in diagram 5.11(b). Although increasing quickly with increasing mass flow rates, especially for the *nosub* design, all plates' pressure losses keep below 200 millibars. Consequently, 0.03 kg/s is an appropriate mass flow rate, both as to heat transfer and as to pressure loss, and all following simulations will apply that value. The heat transfer rate and the resulting temperature spread of the cooling water differ for the different plate designs.
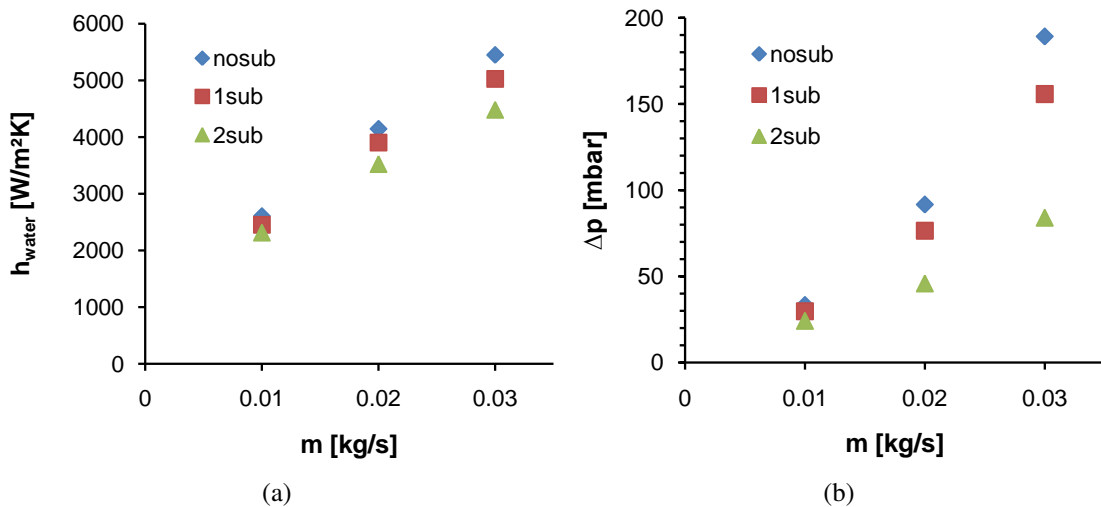

(a)   (b)

Figure 5.11: Prestudy to find the appropriate cooling water mass flow rate

5.5.2 Simulation Results

After having introduced the simulated heat exchanger plate designs and having determined the necessary cooling water mass flow rate in the previous subsections, we can present and discuss the simulation results in this subsection. But before, let us mention the input data:

The cooling water has an inlet temperature of 30 degrees Celsius and an inlet pressure of three bars, at a mass flow rate of 0.03 kilogram per second. As it will do in countercurrent operation, the cooling water flows upwards - the CFD-model considers gravity. On the vapor side, the temperature is 40 degrees Celsius and the heat transfer coefficient between film and plate is assumed constant, 1000 W/m^{2}K. The SolidWorks material database provides the thermal conductivity of the steel plate, which is 15 W/(m·K) for the temperature range in our application.

With that input data, the simulations yield the results presented on the following pages. First, consider the averaged conductive heat transfer coefficients in the water channels of the different plates, shown in figure 5.12. As seen earlier, the designs with a 72.2 degrees channel angle, namely the *nosub*, *1sub* and *2sub* designs, reach an h$_c$ of more than 4000 W/m^{2}K, with *1sub* almost reaching 5000 and *nosub* even exceeding 5000 W/m^{2}K. In contrast, the current *hb* design reaches only 4000 W/m^{2}K and the *nosub63* design slightly more. The latter values however still are sufficient - remember, the aimed convective heat transfer coefficient is 4000 W/m^{2}K. So, as to the averaged convective heat transfer, all designs perform sufficiently. Yet the designs with a 72.2 degree channel angle have a somewhat better heat transfer coefficient.
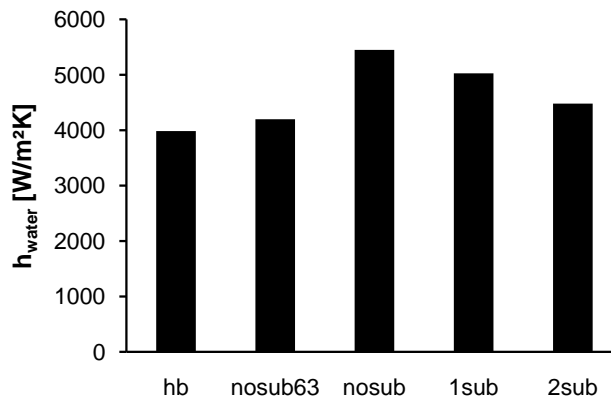

Figure 5.12: Averaged convective heat transfer coefficients on the water side

[Behr (2006)] and [Hulin (2008)] also determined the heat transfer coefficient on the water side of the *hb* heat exchanger. At a 0.03 kilogram per second water mass flow rate, Hulin found a heat transfer coefficient of 8000 W/(m^{2}K), whereas Behr's simulations at m$_c$ = 0.037 kg/s and his calculations at m$_c$ = 0.031 kg/s yielded 1360 and 3260 W/(m^{2}K), respectively. The discrepancy between Behr's and Hulin's values is significant. The result of our simulation of the *hb* heat exchanger, 4000 W/(m^{2}K), is well in

the middle of Behr's lower value and Hulin's value, and close to Behr's higher value. That points on a good feasibility of our value.

Let us now consider the temperature distribution on the vapor side for the respective plate designs, depicted in the figures 5.13-5.17. The plates without subchannels, that is, the *hb*, *nosub 63* and *nosub* design, figures 5.13-5.15, feature a regular pattern of warm spots between the channels. At these spots, the plates are in contact, and thus no cooling water is located between the plates. Consequently the heat absorbed here has to be conducted to the nearest channel before it can be cooled by the water - other than at the rest of the plate, where the heat only has to be conducted through the 0.4 millimeter plate. Because of that longer distance, the thermal resistance between film and cooling water is larger and the temperature on the film side is higher in the respective areas. Thanks to the larger channel angle, the *nosub* plates' contact areas causing the warm spots are somewhat smaller and the distance between them is larger. Hence also the warm spots are smaller and the distance between them is larger compared to the two designs with the 63 degrees channel angle, *hb* and *nosub63*. Moreover the *nosub63* plate shows smaller warm spots than the *hb* plate, because the channel distance is lower. Note that the temperature plots are not true to scale. As stated in section 5.4, the *hb* heat exchanger is 120 millimeters wide and the *nosub63* heat exchanger is 106 millimeters wide, whereas the other heat exchangers are 100 millimeters wide. These differences may, if the beholder is not aware of them, lead to a somewhat wrong impression as to the dimensions of, for instance, the warm spots.

Consider now the temperature plots of the plate pairs with subchannels, the *1sub* and the *2sub* plate packages, shown in the figures 5.16 and 5.17. Here, the warm spots between the channels observed at the previous designs are not present. The temperature differences on the plates are much lower - disregarded the warm edges outside the actual heat exchanger area, where no water channels are present. Obviously the subchannels significantly enhance the plate cooling. Now the warmest spots are located at the intersections of the main channels.
The reason for that new location of the warmest spots can be found in the different convective heat transfer coefficients in the main channels and subchannels. The convective heat transfer coefficients given in figure 5.12 are averaged values. For the *1sub* and *2sub* plates however, there are considerable differences between the heat transfer coefficients in the main channels and in the subchannels: The *1sub* plate shows an averaged convective heat transfer coefficient of 4400 W/m^{2}K in the main channels and 6000 W/m^{2}K in the subchannels, the respective values for the *2sub* plate are 4000 and 5500 W/m^{2}K. Hence, the cooling in the subchannels is more effective than in the main channels and thus the coldest spots are located on the subchannels whereas the warmest spots are located on the main channels. But again, the temperature differences between the cold and the warm spots are comparably low.
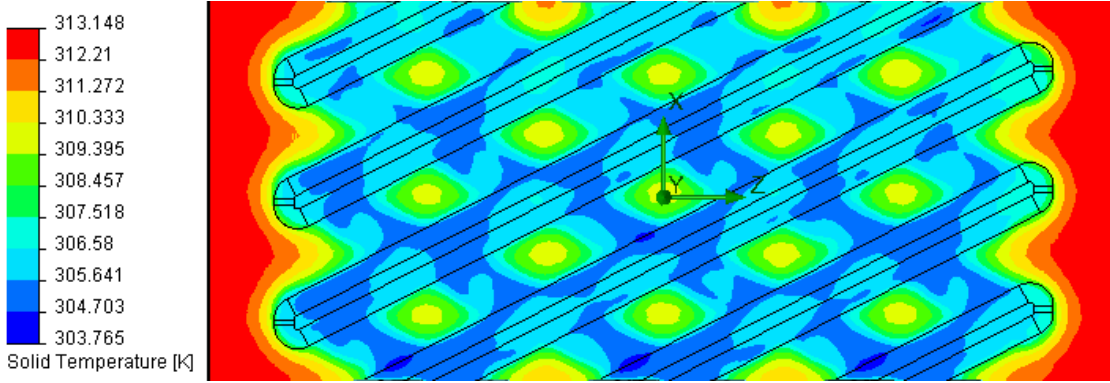
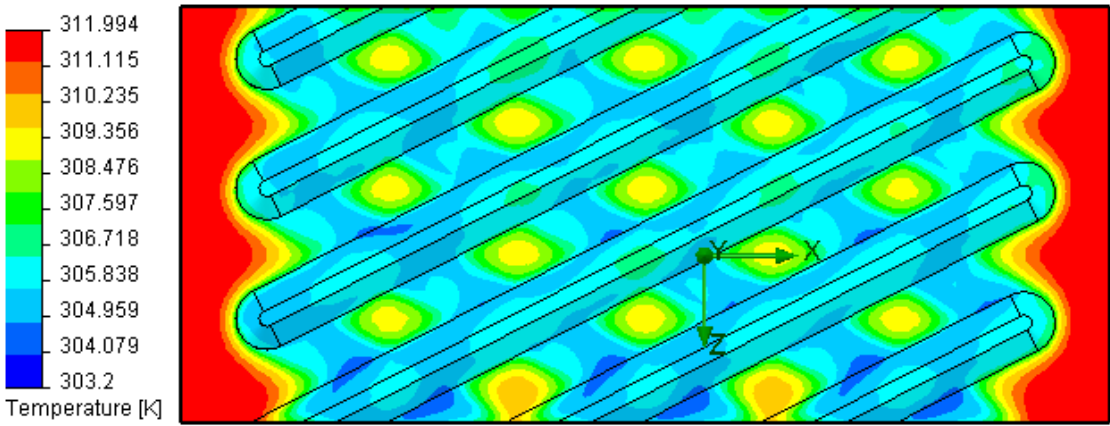**Figure 5.13:** Temperature plot of the film side of the *hb* plate

Figure 5.14: Temperature plot of the film side of the *nosub63* plate
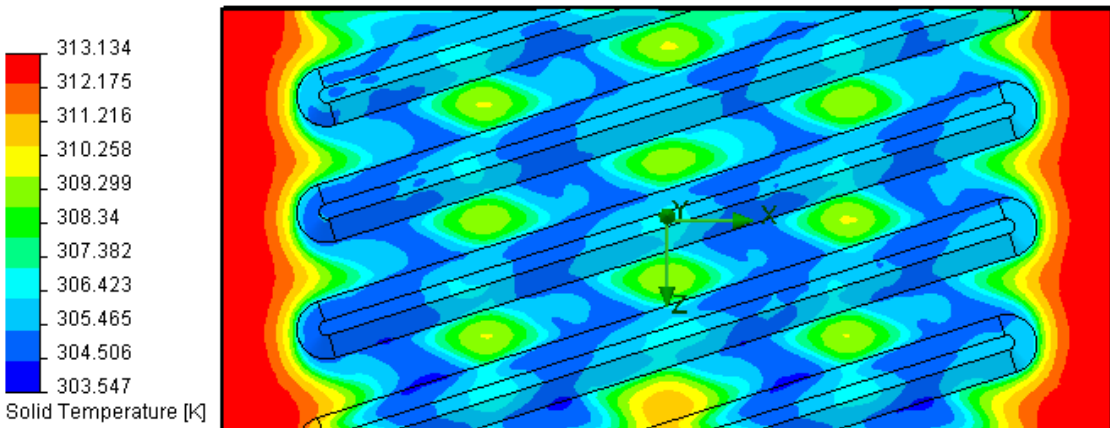

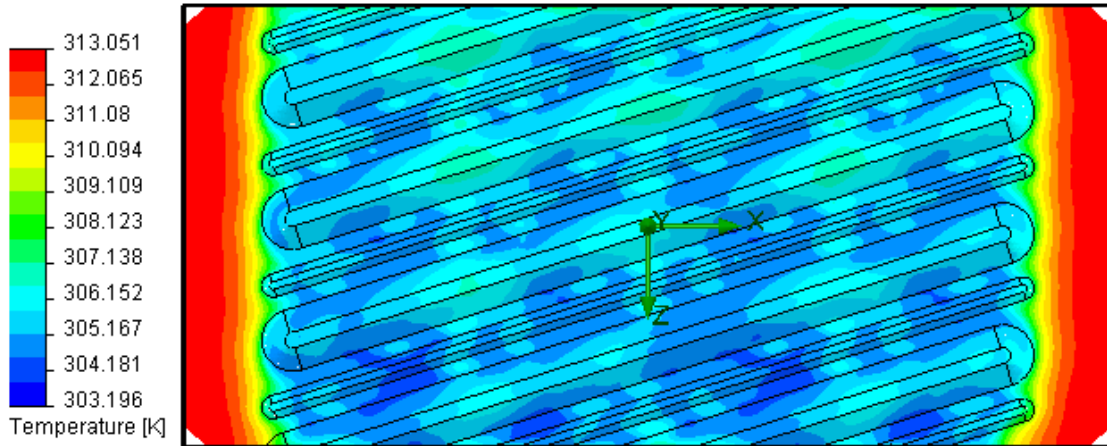**Figure 5.15:** Temperature plot of the film side of the *nosub* plate

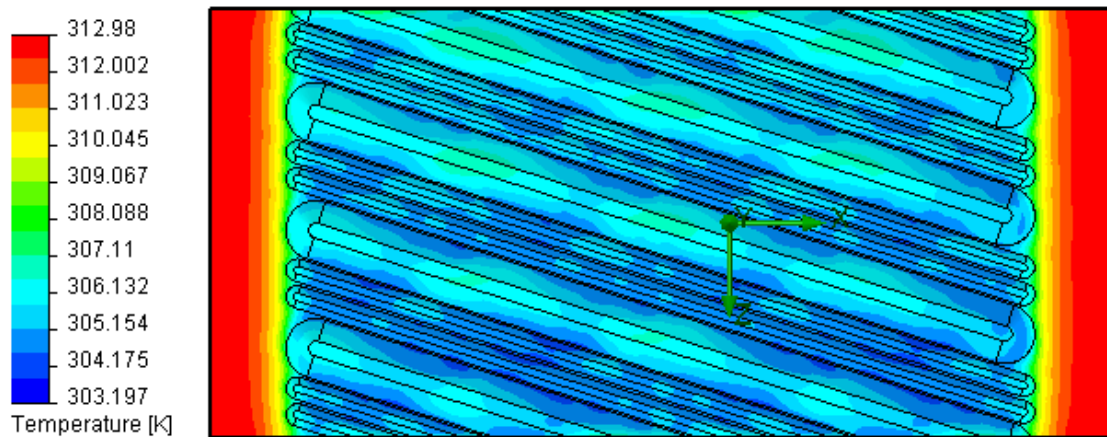**Figure 5.16:** Temperature plot of the film side of the *1sub* plate

Figure 5.17: Temperature plot of the film side of the *2sub* plate

The simulation results so far suggest that the plates with subchannels perform best, yet this evaluation is mainly based on the graphical temperature plots and thus only qualitative. How can we compare the performance of the different designs quantitatively? One major goal in the design of the new heat exchanger is to make the heat exchanger compact. The specific capacity, that is, the heat exchanger capacity per volume, is a measure for the compactness of a heat exchanger. Let us use it to compare the different designs' quality. As mentioned before, the limiting design factor on the water side is the pressure loss, so we take the pressure loss as a second criterion for the evaluation of the heat exchanger designs. Figure 5.18 plots both the specific capacity and the pressure loss of the different plates, assuming that the respective packages are 300 millimeters long.

The *2sub* design achieves the highest specific capacity, some 2500 kW/m^3, at a pressure loss of some 80 millibars, which is well below the defined maximum of 200 millibars. The specific capacity of the *1sub* design is slightly lower, yet the pressure loss is signif-
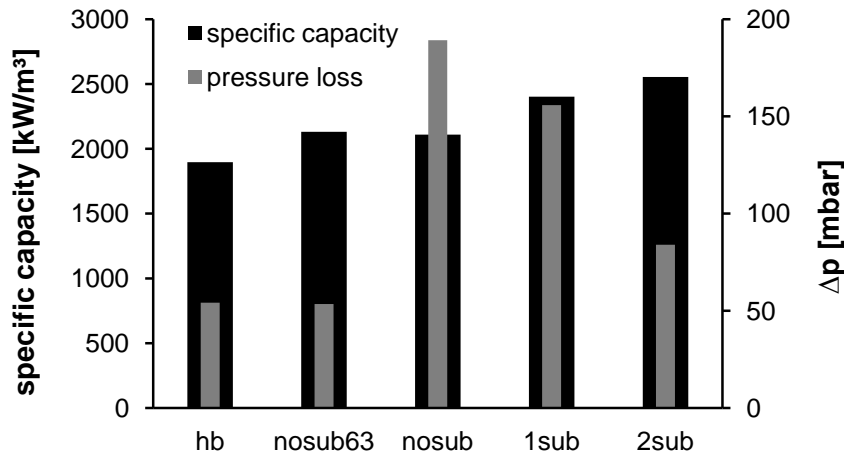
Figure 5.18: Specific capacity and pressure loss of the simulated heat exchanger plates

icantly higher, some 155 millibars - below the 200 millibar limit, however. The *nosub* design has again a somewhat lower specific capacity and a significantly higher pressure loss, just below the 200 millibar limit. Better than the *nosub* design is the *nosub63* design. Its specific capacity is merely slightly higher, but its pressure loss is only somewhat above 50 millibars and hence the lowest of all five designs. The current plate design, the *hb* design, has the lowest specific capacity - it is the only plate below 2000 kW/m^3 - but also has a pressure loss below 60 millibars.

[Behr (2006)] and [Hulin (2008)] determined the pressure loss of the entire *hb* heat exchanger with a 337 millimeter length, also considering the cooling water inlet and outlet openings. Hulin measured a 44 millibar pressure loss at a 0.03 kilogram per second water mass flow rate, Behr simulated at a 0.037 kilogram per second water mass flow rate and found a 48 millibar pressure loss. Our simulations yield a pressure loss below 60 millibars for a 300 millimeter long *hb* heat exchanger package and is hence moderately higher than Behr's and Hulin's results.

5.5.3 Conclusions from the Simulation Results

The results of the CFD-simulations show that different modifications can enhance the specific capacity of the current plate heat exchanger, the *hb* design.

The *nosub63* design is slightly more compact than the *hb* design. The main reason for that is the lower channel distance. First, the lower channel distance results in smaller warm spots on the film side. Second, it increases the heat exchanger area. Third, it reduces the distance between the channel intersections, where turbulence increases because the two intersecting flows have different flow directions. And increased turbulence means increased heat transfer.

In spite, the *nosub63* heat exchanger has a slightly lower pressure loss than the *hb* heat exchanger. As the cross sectional area for the flow is equal for the two designs, the lower pressure loss of the *nosub63* design is due to the lower width of the heat exchanger and

the resulting shorter distance that the cooling water flows in average. The pressure loss however refers to a 300 millimeter-long plate package and as the *nosub63* plate is narrower than the *hb* plate, its heat exchanger area per length is lower. These aspects should be considered when comparing the pressure losses. Nevertheless, the difference of the two designs in terms of pressure loss is so small that it is negligible in praxis.
Assumed that the slightly narrower vapor channels do not affect the vapor flow noteworthy and thus outweigh the advantage of the enhanced cooling, the *nosub63* heat exchanger will perform slightly better than the *hb* heat exchanger. That means, a slight reduction of the channel distance improves the heat exchanger performance.

A comparison of the *nosub63* design with the *nosub* design shows that a mere increase of the channel angle is counterproductive as far as the water side is concerned. The specific capacity of the *nosub* heat exchanger is virtually equal to that of the *nosub63* heat exchanger, yet the pressure loss is more than three times higher. Using the *nosub* design instead of the *nosub63* design only makes sense if the larger channel angle improves wetting on the vapor side, which in turn increases the absorber performance. Then the increased performance justifies the higher pressure loss of the cooling water, which still is below the defined maximum of 200 millibars.

Other than increasing the channel angle, using heat exchanger plates with subchannels both increases the specific capacity and decreases the cooling water pressure loss. The *1sub* plate is equal to the *nosub* plate, yet additionally it has a subchannel between the main channels. This subchannel enhances the specific capacity of the heat exchanger by more than ten percent and reduces the pressure loss by more than ten percent.
Using two subchannels brings a further increase of the specific heat exchanger capacity to 2550 kW/m^3. That means a 35 percent increase compared to the *hb* design and a 21 percent increase compared to the *nosub* design. The pressure loss is 55 percent higher than for the *hb* design but 44 percent lower than for the *nosub* design and hence far below the 200 millibar.
To sum up, subchannels improve the heat transfer and thus the specific capacity of the absorber significantly. They can even compensate for part of the additional pressure loss due to a larger channel angle. Moreover we can expect better wetting on the solution side because of the more sophisticated texture. The somewhat reduced cross section for the vapor flow will not degrade the overall improvements notably.

6 Summary

The present work contributes to the design of a new low-scale absorption chiller based on plate heat exchangers and focuses on improving the plate heat exchanger design. To a minor extent, it covers cycle design. At a capacity of four kilowatts, the planned external temperatures of the absorption chiller are 15/10 degrees Celsius for the chilled water, 30/38 degrees for the cooling water and 90/80 degrees for the hot water.

Integration is a promising approach for an inexpensive and compact heat exchanger design. First, the solution distribution system can be integrated into the plate structure of the heat exchanger. Second, the walls of the pressure vessel around the heat exchanger can be integrated into the heat exchanger plates. Thus, the heat exchanger forms its own vessel and does no longer need a separate one. Third, two heat exchangers can be integrated on one plate.
The latter demands that the heat exchangers be pairwise equal. In contrast to an individual optimization of the heat exchanger areas, an absorption chiller with pairwise equal heat exchangers has a larger overall heat exchanger area. Cycle calculations show, however, that this effect is moderate. The benefit resulting from, among others, reduced manufacture cost, prevails.

Insufficient wetting causes the poor performance of the current heat exchanger prototype when used as absorber. To enhance the solution mass flow rate and thus wetting, two recirculation concepts for the absorber are of interest: Recirculation with mixture in the sump (*sump recirculation*) and recirculation with mixture before the absorber (*mixed recirculation*). According to cycle calculations, both concepts perform similarly. Mixed recirculation is slightly better as to heat exchanger area and COP, yet sump recirculation is easier to carry out and hence the preferable concept.
To overcome poor wetting at the generator, a thinkable approach is pool boiling. But the results of the respective cycle calculations indicate that a pool generator does not work with the planned external temperatures. To operate a pool generator, at least one of the external temperature levels needs to be adopted - a compromise is to be found.

As to the heat exchanger, three design changes are considered: First, creation of smaller subchannels between the existing channels to enhance wetting, second, reduction of the heat exchanger width to reduce the vapor pressure loss, and third, increase of the channel angle, also to reduce the vapor pressure loss.
A CFD-based comparison of five design variants gives information on the impact of different plate design changes. As could be expected, the heat exchanger width has little impact on the water side. At a constant water mass flow rate, a lower heat exchanger width causes a faster water flow and thus enhances the heat transfer slightly.

Additionally reducing the channel distance compensates for the increased pressure loss. In contrast, an increased channel angle is negative for the water side. Though hardly impacting the specific capacity of the heat exchanger, it causes a strong increase of pressure loss, which could only be justified by significant improvements on the vapor side, as for instance enhanced wetting or reduced vapor pressure loss.

The most effective of the considered design changes are subchannels, smaller channels between the main water channels. In addition to their expected positive influence on wetting with solution, subchannels both reduce the water pressure loss and enhance the heat transfer, resulting in a high specific capacity. That positive effect is even stronger with two subchannels between two main channels.

Prosecution of the Project

After having investigated different design changes' impact on the water side of the heat exchanger, the next step in the ZAE Bayern project *Absorptionskältemaschine auf Basis kompakter Plattenapparate* is to design, manufacture and conduct tests with a new heat exchanger prototype. Consultations with the industrial project partner have to show how exactly the design ideas can be realized. Tests of the new heat exchanger prototype will show to what extent the planned design changes result in the anticipated performance enhancement. If the new heat exchanger design proves to work in the desired way, an absorption chiller prototype can be designed and tested.

So far, the project focused on the absorber and generator. A further task will be to design the evaporator and the condenser. Moreover, the final cycle design has to be found, as well as the external temperatures. Eventually, the project may result in the prototype of an absorption chiller with potential to challenge the established low-scale vapor-compression chillers.

References

[Alefeld & Radermacher (1993)]   **G. Alefeld, R. Radermacher:** *Heat Conversion Systems.* ISBN 0-8493-8928-3, CRC Press, Boca Raton 1993.

[Alfa Laval (2004)]   **Alfa Laval:** *Brazed heat exchangers. A product catalogue for refrigeration.* http://www.alfalaval.com/solution-finder/products/ac-series/pages/documentation.aspx?Source=http%3a%2f%2fwww.alfalaval.com%2fsolution-finder%2fproducts%2fpages%2fdefault.aspx%3ftype%3dProductCategory%26firstItemID%3d54e32261-aa20-4f0f-9851-344c49bf67b7 (accessed on May/13/2011).

[Behr (2006)]   **C. Behr:** *Wärme- und Stoffübertragung an einem Absorber in Plattenwärmeübertrager-Ausführung einer Absorptionskältemaschine.* Diploma thesis, Fachhochschule München, Munich 2006.

[Beil (2011)]   **A. Beil:** *Entwicklung eines Teststandes zur Untersuchung neuartiger Plattenwärmetauscher als Hauptkomponenten für Absorptionskältemaschinen.* Bachelor thesis, Fachhochschule Deggendorf, Munich 2011.

[Bethge & Wüst (2007)]   **P. Bethge, C. Wüst:** *Zeit für eine Revolution.* DER SPIEGEL 7/2007, ISSN 0038-7452, SPIEGEL-Verlag Rudolf Augstein, Hamburg 2007.

[Clausen (2007)]   **J. Clausen:** *Zukunftsmarkt Solares Kühlen.* Fallstudie im Auftrag des Umweltbundesamtes im Rahmen des Forschungsprojektes Innovative Umweltpolitik in wichtigen Handlungsfeldern, Förderkennzeichen 206 14 132/05. Borderstep Institut, ISSN 1865-0538, Karlsruhe 2007.

[Estiot et al. (2007)]   **E. Estiot, S. Natzer, C. Schweigler:** *Heat Exchanger Development for Compact Water/LiBr Absorption Systems.* Proceedings of the 22nd IIR International Congress of Refrigeration, Beijing 2007.

[Estiot (2009)]   **E. Estiot:** *Behältersieden von wässriger Lithi-umbromidlösung - Untersuchung zur Entwicklung kompakter Absorptionskältemaschinen.* PhD thesis, Technische Universität München, ISBN 978-3-86853-385-9, Verlag Dr. Hut, Munich 2009.

[Gorenflo (2006)]   **D. Gorenflo:** *Behältersieden (Sieden bei freier Konvektion).* VDI-Wämeatlas, 10. Auflage. Verein Deutscher Ingenieure, Springer-Verlag, Berlin/Heidelberg 2006. Chapter Hab.3.

[Herold et al. (1996)]   **K.E. Herold, R. Radermacher, S.A. Klein:** *Absorption Chillers and Heat Pumps.* ISBN 0-8493-9427-9, CRC Press, Boca Raton 1996.

[Höges (1997)]   **V. Höges:** *Klimatisierter Alptraum. Wie sich die Amerikaner bemühen, die größten Energiever-schwender der Welt zu bleiben.* DER SPIEGEL 49/1997, ISSN 0038-7452, SPIEGEL-Verlag Rudolf Augstein, Hamburg 1997.

[Hulin (2008)]   **S. Hulin:** *Wärmeübertragung und Druckverlust eines Plattenwärmetauschers für eine Absorption-skältemaschine.* Diploma thesis, Technische Universität München, Munich 2008.

[Joudi & Lafta (2000)]   **K.A. Joudi, A.H.Lafta:** *Simulation of a simple absorption refrigeration system.* Energy Conversion and Management, Vol.42, pp. 1575-1605, 2001.

[Jung (2007)]   **A. Jung:** *Why Conservation Is the World's Best Energy Source.* SPIEGEL ONLINE, November 2007. http://www.spiegel.de/international/world/0,1518,476231,00.html (accessed on May/7/2010).

[Kaji et al. (1995)]   **M. Kaji, M.Furukawa, T. Suyama, K. Sekoguchi:** *Enhancement of Pool Boiling Heat Transfer to Lithium Bromide Aqueous Solution.* Technology Reports of the Osaka University, Vol.45, pp.49-58, April 1995.

[Kommer & Hinz (2010)]   **C. Kommer, C. Hinz:** *DSW-Datenreport 2010. Soziale und demographische Daten zur Weltbevölkerung.* Deutsche Stiftung für Weltbevölkerung, ISBN 3-930406-10-1, Hannover 2010.

[Lee et al. (1991)]   **C.C. Lee, Y.K. Chuah, D.C. Lu, H.Y. Chao:** *Experimental investigation of Pool Boiling of Lithium Bromide Solution on a Vertical Tube under Subatmospheric Pressures.* International Communications in Heat and Mass Transfer, Vol.18, pp. 309-320, 1991.

[Martin (2006)]   **H. Martin:** *Druckverlust und Wärmeübergang in Plattenwärmeübertragern.* VDI-Wärmeatlas, zehnte Auflage, Springer-Verlag, Berlin Heidelberg 2006.

[Natzer et al. (2010)]   **S. Natzer, M. Walch, C. Schweigler:** *Unterstützung von trockener Rückkühlung: Vorkühleffekt bei Installation in Tiefgeschossen.* Deutsche Kälte-Klima Tagung, Magdeburg 2010.

[Parsons & Forman (1989)]   **R.A. Parsons, C. Forman:** *ASHRAE Handbook of Fundamentals.* ISBN 0-9101-1056-5, American Society of Heating, Refrigerating and Air Conditioning Engineers, Inc., 1989.

[Plura (2008)]   **S. Plura:** *Entwicklung einer zweistufigen Absorptionkältemaschine zur effizienten Kraft-Wärme-Kältekopplung.* PhD thesis, Technische Universität München, Munich 2008.

[Riesch (1991)]   **P. Riesch:** *Wärmetransformatoren mit hohem Temperaturhub.* PhD thesis, Technische Universität München, Munich 1991.

[Schweigler (1999)]   **C. Schweigler:** *Kälte aus Fernwärme - Konzept, Auslegung und Betrieb der Single-Effect/Double-Lift-Absorptionskälteanlage.* Fortschritt-Berichte VDI, Reihe 19, Nr. 121, ISBN 3-18-312119-0, VDI Verlag, Düsseldorf 1999.

[Uemura & Hasaba (1964)]   **T. Uemura, S. Hasaba:** *Studies on the lithium bromide-water absorption refrigeration machine.* Technology reports of Kansai University, Vol.6, pp. 31-55, 1964.

[Versteeg & Malalasekera (1995)]   **H.K. Versteeg, W. Malalasekera:** *An introduction to Computational Fluid Dynamics - The Finite*

Volume Method. ISBN 978-0-582-21884-0, Pearson Education Limited, Essex 1995.

[Wuschig (2007)]   **C. Wuschig:** *Modellierung und Bewertung von angepassten zwei-/einstufigen LiBr/H_2O - Absorptionsmaschinen.* Diploma thesis, Technische Universität München, Munich 2007.

[Wuschig et al. (2009)]   **C. Wuschig, S. Plura, C. Schweigler:** *Optimierung von Absorptionskältemaschinen.* KI Kälte Luft Klimatechnik, pp. 28-33, July/August 2009.

A   Solution Mass Flow Rate for Good Wetting

Good wetting is crucial for an absorber to perform well. [Beil (2011)] conducted wetting tests with a plastic model plate pair of the current plate heat exchanger, the *hb* design. He found that aqueous lithium-bromide solution starts to wet the surface at a minimum volume flow rate of 0.15 liters per minute. Good wetting requires 0.4 liters per minute. To assure that the volume flow rate is sufficient for complete wetting, let us assume a volume flow rate of $\dot{V} = 0.5$ liters per minute or $8.333 \cdot 10^{-3}$ liters per second, respectively.

The plates are 356 millimeters high and 120 millimeters wide, so the approximate surface area of one plate is

$$A_p \approx 0.356\ m \cdot 0.120\ m = 4.272 \cdot 10^{-2}\ m^2. \tag{26}$$

Consisting of two plates, the package area to be wetted is

$$A_w = 2 \cdot A_p = 8.544 \cdot 10^{-2}\ m^2. \tag{27}$$

With the aqueous lithium-bromide solution's density $\rho = 1.5$ kilogram per liter, the required mass flow rate writes

$$m = \dot{V} \cdot \rho = 8.333 \cdot 10^{-3} \frac{l}{s} \cdot 1.5 \frac{kg}{l} = 1.25 \frac{kg}{s}. \tag{28}$$

Finally, dividing the required mass flow rate with the wetted area yields the specific mass flow rate

$$\frac{m}{A_w} = \frac{1.25 \frac{kg}{s}}{8.544 \cdot 10^{-2}\ m^2} = 0.146 \frac{kg}{m^2 s}. \tag{29}$$

The cycle calculations considering solution recirculation at the absorber - see chapter 4 - prescribe that value to justify the assumption of complete wetting. For different plate dimensions or a different heat exchanger pattern, respectively, the required specific mass flow rate will differ.